ORIGINAL ARTICLE

FISH and FISHERIES WILEY

Latitudinally distinct stocks of Atlantic cod face fundamentally different biophysical challenges under on-going climate change

Olav Sigurd Kjesbu[1] | Maud Alix[1] | Anne Britt Sandø[1,2] | Espen Strand[1] | Peter J. Wright[3] | David G. Johns[4] | Anders Thorsen[1] | C. Tara Marshall[5] | Kjell Gunnar Bakkeplass[1] | Frode B. Vikebø[1] | Mari Skuggedal Myksvoll[1] | Geir Ottersen[6,7] | Bridie J. M. Allan[1] | Maria Fossheim[8] | Jan Erik Stiansen[1] | Geir Huse[1] | Svein Sundby[1]

[1]Institute of Marine Research, Bergen, Norway

[2]Bjerknes Centre for Climate Research, Bergen, Norway

[3]Marine Scotland Science, Aberdeen, UK

[4]Citadel Hill Laboratory, Continuous Plankton Recorder Survey, Marine Biological Association, Plymouth, UK

[5]School of Biological Sciences, University of Aberdeen, Aberdeen, UK

[6]Institute of Marine Research, Oslo, Norway

[7]Centre for Ecological and Evolutionary Synthesis, Department of Biosciences, University of Oslo, Oslo, Norway

[8]Institute of Marine Research, Tromsø, Norway

Correspondence
Olav Sigurd Kjesbu, Institute of Marine Research, PO Box 1870 Nordnes, NO-5817 Bergen, Norway.
Email: olav.kjesbu@hi.no

Present address
Peter J. Wright, Marine Ecology and Conservation Consultancy, Ellon, UK
Bridie J. M. Allan, University of Otago, Dunedin, New Zealand

Funding information
Havforskningsinstituttet; Norges Forskningsråd, Grant/Award Number: 133836/120; Norwegian Fisheries Research Sales Tax System, Grant/Award Number: 15205; Scottish Government, Grant/Award Number: SP009; Trond Mohn stiftelse, Grant/Award Number: BFS2018TMT01; CPR Survey

Abstract

The reproductive success of marine ectotherms is especially vulnerable in warming oceans due to alterations in adult physiology, as well as embryonic and larval survival prospects. These vital responses may, however, differ considerably across the species' geographical distribution. Here we investigated the life history, focusing on reproductive ecology, of three spatially distant populations (stocks) of Atlantic cod (*Gadus morhua*, Gadidae) (50–80° N), in the Irish/Celtic Seas-English Channel Complex, North and Barents Seas, under past and projected climate. First, experimental tracking of spawning behaviour evidenced that the ovulation cycle is highly distressed at ≥9.6 (±0.25)°C (T_{up}). This knife-edge threshold resulted in erratic spawning frequencies, whereas vitellogenin sequestration remained unaffected, indicating endocrine rather than aerobic scope constraints. Cod in the Celtic Sea-English Channel are, therefore, expected to show critical stock depensation over the next decades as spawning grounds warm above T_{up}, with Irish Sea cod subsequently at risk. Second, in the relatively cooler North Sea, the northward retraction of *Calanus finmarchicus* (Calanidae) and *Para-Pseudocalanus* spp. (Clausocalanidae) (1958–2017) limit cod larvae feeding opportunities, particularly in the southernmost subarea. However, the contrasting increase in *Calanus helgolandicus* (Calanidae) does not counteract this negative effect, likely because cod larvae hatch ahead of its abundance peaks. Overfishing again comes as a twin effect. Third, in the still relatively cold Barents Sea, the sustainably harvested cod benefit from improved food conditions in the recent ice-free polar region but at the energetic cost of lengthier and faster spawning migrations. Consequently, under climate change local stocks are stressed by different mechanistic factors of varying management severity.

KEYWORDS
aerobic scope, larvae, ovulation, RCP 4.5, recruitment, spawning

1 | INTRODUCTION

The iconic Atlantic cod (*Gadus morhua*, Gadidae) (Jakobsson et al., 1994; Kurlansky, 2011) is managerially split into approximately twenty major stocks across the North Atlantic (Brander, 2005; Marteinsdottir & Rose, 2019). Local cod stocks are, therefore, subject to highly different living conditions at both sides of the North Atlantic (Brander, 2005; Sundby, 2000) and will be even more so under on-going anthropogenic climate change (IPCC, 2021) (Figure 1). Earlier synopses of this generally well-studied gadoid have provided important insights about the potential consequences of changing climate on its biology and harvestable surplus production; such integration efforts might help with deciphering local responses to climate change as these can be clearly stock dependent (Brander, 2019; Kjesbu et al., 2022). For instance, the impact of key environmental factors, such as temperature (*T*), on stock productivity is known to vary substantially across ocean basins (Drinkwater, 2005; Planque & Frédou, 1999). Southern stocks appear less productive under higher-than-normal *T* (Drinkwater, 2005; Pershing et al., 2015), whereas northern stocks do comparatively better (Drinkwater, 2005; Kjesbu et al., 2022), provided they are sustainably harvested (Kjesbu et al., 2014). Moreover, both the spawning cycle and early life-history survival of this species have in recent expert scorings been listed as particularly sensitive to warming waters (Kjesbu et al., 2022). Hence, these sensitivity attributes were presently hypothesized as 'the weak link in the chain'. To specifically highlight their local modes of action and consequences, we undertook an in-depth mechanistic investigation, encouraged by access to extremely rich data sources, including for the associated biophysical drivers.

Generally, warming directly impacts teleost physiology (Little et al., 2021), where the most sensitive stages, corresponding to the narrowest thermal windows of tolerance, refer to spawners and their embryos (Dahlke et al., 2020; Pörtner & Farrell, 2008). Indeed, reproductive failure at spawning accelerates at higher-than-optimal temperatures in several fish species, manifested as a shift in or even an inhibition of the spawning season and decline in reproductive success (Alix et al., 2020; Miranda et al., 2013). To describe and understand the fundamental mechanisms involved in the reproductive response (spawning performance) of adults facing variations in temperature, the oxygen- and capacity-limited thermal tolerance (OCLTT) theory offers an explanation (Pörtner et al., 2008, 2017). The key principle within the OCLTT theory is that the scope for aerobic performance of a given physiological rate (or speed) follows a bell-shaped curve as a function of body temperature (Pörtner et al., 2008, 2017), in ectotherms reflecting ambient *T* (Levesque & Marshall, 2021). This thermal performance curve might be less clear at the molecular level (Pörtner et al., 2017). Anyhow, a performance optima (T_{opt}) is a mandatory criterion of the OCLTT, implying a lower tolerance outside this window, represented by lower (T_{lp}) and upper pejus *T* (T_{up}), and, ultimately, critical *T*s with near zero performance (Pörtner et al., 2017; Pörtner & Farrell, 2008). However, early life-history stages can also be negatively influenced by ocean warming in indirect ways, even at $T \ll T_{up}$, where alternations in zooplankton

(larval prey) biography stand out as one of the prime candidates for study (Beaugrand et al., 2003). Besides, the distribution of mid- and high-latitude species is typically displaced polewards during global warming (Morley et al., 2018; Poloczanska et al., 2013). Therefore,
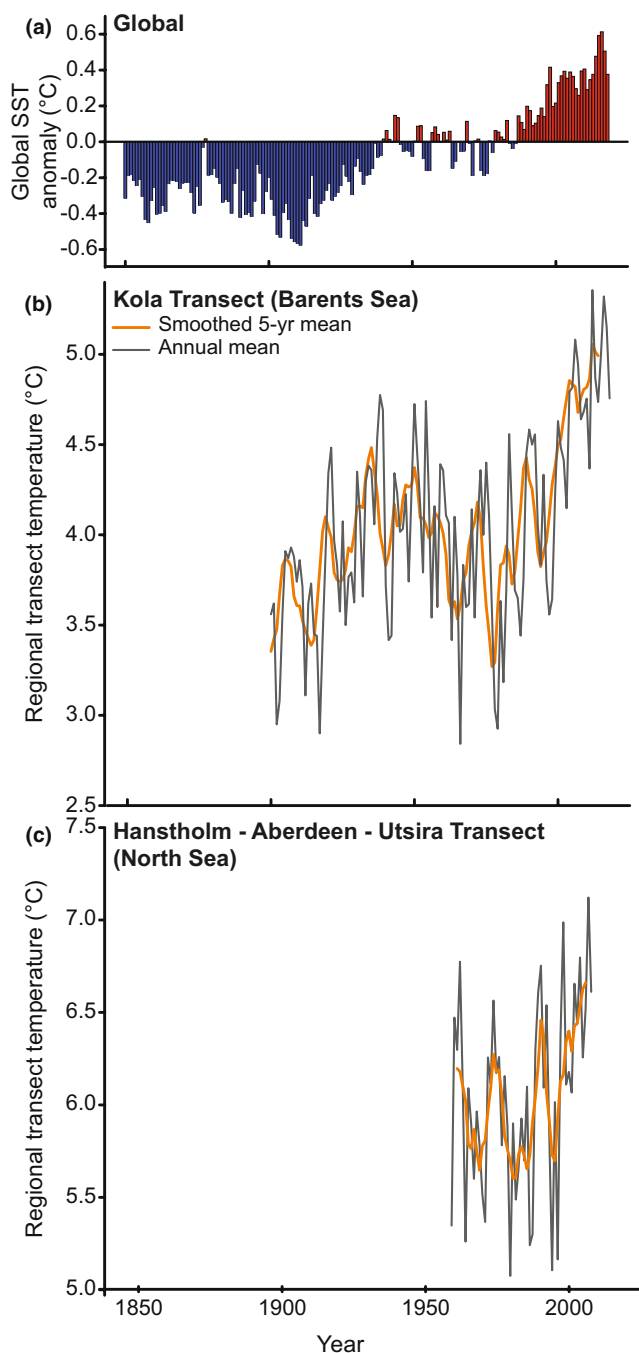
FIGURE 1 Long-term trends in global and regional temperature. (a) Global sea surface temperature (SST) anomalies (1850–2018); (b) regional transect temperature in the Barents Sea (0-200m, 1900–2018) and (c) North Sea (0-100m, 1958–2008).

FIGURE 2 Change in temperature from 1987 to 2002 in the sea-water inlet at the experimental facility in Bergen, Norway. A 'warm wave' (see main text) was detected in 2002, briefly transient in 2001, whereas undetectable in 2000. The years 1987, 1991 and 1997 were added for further comparison. All temperature measurements were taken near the surface within the same tank (spawning chamber 8 (Kjesbu, 1989)).

North (5–7°C) and Barents Seas (4–6°C), though conspecifics on the other side of the Atlantic, for example Northern cod, may spawn near 0°C (Brander, 2005). This spectrum of spatially diverging environmental conditions was used to contextualize the likely future performance of spawners and early life-history stages that govern local cod recruitment dynamics and, ultimately, their future productivity (Kjesbu et al., 2022; Payne et al., 2021) and management (Gullestad et al., 2020; Payne et al., 2021). Within the framework of on-going (Figure 1) and projected climate change (as specified below), our objectives were to (i) precisely and accurately define temperatures at which reproductive failure takes place in Atlantic cod and explore the underlying physiological modes of action, with particular reference to reproductive investment (oocyte growth) and egg release coinciding with natural 'warm waves' (i.e., seeing relatively extreme environmental temperatures over a limited period of time) as detected in experimental facilities (Figure 2); (ii) identify cod stocks likely to be subject to such detrimental thermal impacts and (iii) determine other specific factors that may limit cod future reproductive success in this marine realm, placing special emphasize on fine-scale changes in zooplankton biography but also any heightened migration costs. To do so, this article critically revisits earlier concepts and findings, supported by unique experimental and field time series data.

2 | MATERIALS AND METHODS

To synthetize a greater understanding of the reproductive ecology of Atlantic cod in view of climate change, multiple streams of data and models were utilized, as summarized in Table 1 and specified in the below M&M sections. A complete List of Abbreviations and Terms appears in Appendix S1.

although T_{up} is a sensible target for causal studies, the chains of eco-physiological reactions might be far more complicated. Furthermore, general principles developed for a species might be less relevant at the local population level, either because the detrimental effect attributed to climate change is much stronger, or, at other end of the scale, not yet detectable.

We targeted three Atlantic cod stocks experiencing close to the maximum range in spawning T in the Northeast Atlantic, that is cod located in the Irish/Celtic Seas-English Channel Complex (6–9°C),
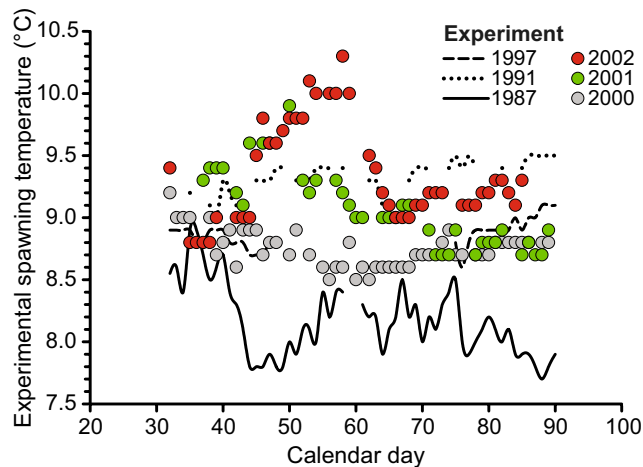
TABLE 1 'Roadmap' of consulted data, models and internet web links within each of the four main research topics. Further details and references are given in the main text of the Material and Methods section

Topic	Type of data, model or web link
Cod reproductive physiology	
Vitellogenin uptake	**Field females**: A random sub-set of 300 fecundity females of Barents Sea cod from commercial landings (N = 796, vitellogenic or final maturation stage): 1986, 1988, 1989, 1999–2001, 2003–2006
	Experimental females: 24 Barents Sea cod females sampled by IMR research vessels and held in spawning chambers, each 'paired' with one male: 2000, 2001 and 2002 (320 egg batches) (Table S1)
Spawning frequency	**Experimental females**: 19 Barents Sea cod females (same material as above) where all batches (N = 267, 8.2–10°C) showed at least some fertilized eggs; similar data from 15 Coastal cod South females (4.1–8.3°C) (Kjesbu, 1989), and aggregated, tabled data per female on 38 Gulf of St Lawrence cod females (held at either 2 or 4–5°C) (Ouellet et al., 2001)
Embryos	**Experimental females**: 5 Barents Sea cod females (same material as above) experiencing different max temperatures (9.1–10.3 °C) during spawning, studying the immediate effect on egg fertilization rate, egg dry weight and egg batch production
Climate impacts on cod spawning ground persistence	
Observed trends in global and regional temperature	**Global**: Met Office Hadley Centre, UK, **1850–2018**
	Barents Sea: Kola Transect Section, VNIRO, Russia, **1900–2018**
	North Sea: Hansholm-Abderdeen, Utsira-Start Point, IMR, **1958–2008**
Fate of southern cod spawning grounds	**RCP 4.5**, ROMS/CORE2/SODA/NorESM1-M, **2006–2070**
Larval prey and recruitment proxies for North Sea cod	
Variation in copepod abundance	**CPR data**: *Calanus finmarchicus*, *C. helgolandicus* and *Para-Pseudocalanus* spp. abundance: CPR Survey, UK, **1958–2017**
Variation in copepod abundance in subareas	Same material as above, split by Southern/Northwestern/Viking4a
Spawning stock biomass and recruits	
Whole North Sea	**Stock metrics** (SSB, recruitment): ICES (2015), **1960–2017**
	Surface temperature: NOAA web link, USA, **1958–2020**
	Transect temperature: as above
	Copepod abundance: as above
North Sea subareas	**Stock metrics** (SSB, recruitment): IBTS Q1 and Q3, **1978–2018**
	Copepod abundance: see above
Spawning migration dynamics of Barents Sea cod	
Centre of gravity	**Winter Survey** (February–March), Norway/Russia: **1981–2017**
	Ecosystem Survey (August–September), Norway/Russia: **2004–2017**
	CTD data (in situ temperature): IMR, from the same survey series
	Kola Transect temperature (see above): restricted to **1981–2017**
Displacement distance and directional speed	**Kola Transect temperature** (see above): restricted to **2004–2017**
	Ice extent: Norwegian Polar Institute, restricted to **1981–2017/2004–2017**
	Suitable feeding area: IMR, **1981–2017**
	Total stock biomass: ICES (2020), restricted to **1981–2017/2004–2017**
	Distance estimation: GeeksforGeeks web link

2.1 | Cod reproductive physiology

2.1.1 | Vitellogenin uptake

This analysis was designed to specifically test if the reproductive investment (and thereby the oxygen demand) becomes heightened during spawning, that is when the gonad peaks in size, especially in larger specimens (Pörtner & Farrell, 2008). Individual reproductive investment was represented by the daily, overall, dry weight-based uptake of yolk (vitellogenin) ($\Delta VDW_{overall}$). The established series of equations (Table 2)—given from the observed material on **field and experimental females** (Table 1)—therefore, ultimately aimed at accurately quantifying and contrasting $\Delta VDW_{P, overall}$ (P = pre-spawning) (Table 2, Equation 7) and $\Delta VDW_{S, overall}$ (S = spawning)

TABLE 2 Equations used to estimate reproductive investment in Barents Sea cod. Each equation—with its number, parameters and mathematical expression—is placed under either the pre-spawning (field), spawning (experimental) or model simulation study

EQ.	Parameters	Expression
Field females—Landed data on pre-spawning cod		
1	Potential, pre-spawning fecundity (F_P, in million) vs. total length (TL, in cm) and	$F_P = 3.05 \times 10^{-7} \times TL^{3.591}$ ($N = 300$; $r^2 = 0.834$, $p < .001$)
2	The corresponding whole-body weight (W, in g)	$W = 3.72 \times 10^{-3} \times TL^{3.200}$ ($N = 300$; $r^2 = .968$, $p < .001$)
3	Mean vitellogenic diameter (MOD, in μm) vs. leading cohort diameter (LC, in μm) and	$MOD = 0.932 \times LC - 51.4$ ($r^2 = .952$, $p < .001$; $250 < LC < 800\,\mu m$)
4	The corresponding dry weight (VDW_{MOD}, in μg)	$VDW_{MOD} = 0.1613 \times (19 + 0.947 \times MOD) - 52.3$ ($r^2 = .974$, $p < .001$)
5	Length of vitellogenic period (VP, in days) vs. MOD and temperature (T, in °C) and	$VP = (MOD - 250)/(4.21 \times 1.44^{(T - 9.60)/10})$
6	The corresponding daily increase in oocyte dry weight (ΔVDW_P, in μg day^{-1}) and	$\Delta VDW_P = VDW_{MOD}/VP$
7	The corresponding figure for all oocytes prior to spawning ($\Delta VDW_{P,\,overall}$, in g day^{-1})	$\Delta VDW_{P,\,overall} = \Delta VDW_P \times F_P$
Experimental females—tank data on spawning cod		
8	Pre-spawning, total egg dry weight ($TEDW_P$, in g), where F_R (in million) is realized fecundity	$TEDW_P = VDM_{MOD} \times F_R$
9	The corresponding complete investment ($TEDW_{P+S}$, in g) and	$TEDW_{P+S} = WEDW \times F_R$
10	The corresponding investment attributed to spawning only ($TEDW_S$, in g) and	$TEDW_S = TEDW_{P+S} - TEDW_P$
11	The corresponding rate ($\Delta VDW_{S,\,overall}$, in g day^{-1}), where SP is spawning period (in days)	$\Delta VDW_{S,\,overall} = TEDW_S/SP$
Experimental females—further preparation for the model simulation		
12	Number of egg batches (N_B) shed as a function of F_R	$N_B = 11.76 \times F_R^{0.290}$ ($N = 24$, $r^2 = .621$, $p < .001$)
13	Batch fecundity (F_B, in thousand) as a function of F_P and N_B	$F_B = 1000 \times F_P/N_B$
14	Weighted mean egg dry weight ($WEDW$, in μg) as a function of W	$WEDW = 5.23 \times 10^1 \times W^{0.065}$ ($N = 23$, $r^2 = .370$, $p = .002$, $35 \leq TL \leq 79\,cm$)
Model simulation		
15	Spawning frequency (S_f) as function of T	$S_f = (1/62) \times 1.98^{(T - 8.0)/10}$
16	Spawning interval (between egg batches) (SI, in h) as a function of S_f and	$SI = 1/S_f$
17	The corresponding daily increase in oocyte dry weight (ΔVDW_S, in μg day^{-1}) and	$\Delta VDW_S = (WEDW - VDW_{LC})/(SI/24)$
18	The corresponding $\Delta VDW_{S,\,overall}$ (in g) for all oocytes, consulting F_B (in thousand)	$\Delta VDW_{S,\,overall} = F_B \times \Delta VDW_S/1000$

(Table 2, Equation 11). Furthermore, the latter estimate functioned as ground-truthing (validation) in the subsequent **model simulation** (Table 2, Equation 18) on standardized reproductive and body size data sets.

Field females, collected off northern Norway (69–71° N) over twenty years (1986, 1988, 1989, 1999–2001, 2003–2006), were measured for total length (TL, in cm), whole-body weight (W, in g) and whole ovary weight (OW, in g). All of the presently considered specimens were Barents Sea cod ($N = 796$; $50 \leq TL \leq 135\,cm$) according to otolith zonal patterns (Rollefsen, 1934). Their potential fecundity (F_P) was determined in the laboratory from buffered formaldehyde-preserved subsamples, for the first three study years by the gravimetric method (Kjesbu et al., 1998) and later on by advanced image analysis, that is the auto-diametric method (Thorsen & Kjesbu, 2001).

For exploratory consistency, 30 randomly selected individuals were analysed for F_P per sampling year (Figure 3a; Table 2, Equation 1). The matching equation for W versus TL was given (Table 2, Equation 2). The 10%-largest developing (vitellogenic) oocyte diameter, named the leading cohort (LC, in μm), precisely defined individual maturity status (Thorsen & Kjesbu, 2001). Mean diameter of the corresponding whole vitellogenic oocyte distribution (mode) (MOD, in μm) was established as a function of LC (Figure 3b; Table 2, Equation 3), estimating thereafter the typical dry weight (VDW_{MOD}, in μg), accounting for the slight effect of oocyte diameter swelling in formaldehyde fixation (Thorsen & Kjesbu, 2001) (Table 2, Equation 4). About 85% of VDW_{MOD} was considered vitellogenin, the remaining part being eggshell (chorion) material (Plack et al., 1971; Thorsen et al., 1996). Time of initiation of the reproductive cycle (vitellogenesis), that is
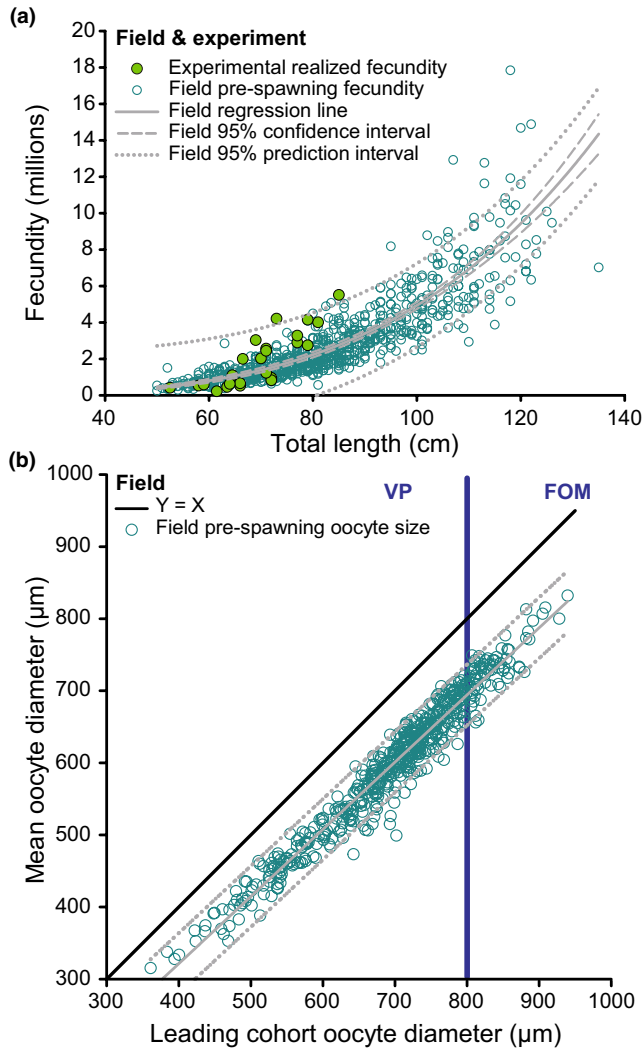
FIGURE 3 Pre-spawning investment in Barents Sea cod. (a) Fecundity of field and captive Barents Sea cod as a function of total length. The field specimens—providing pre-spawning (potential) fecundity—were landed in northern Norway between 1986 and 2006 (totally 10 years), whereas the captive specimens—providing realized fecundity—were held in separate spawning chambers, with one female and male in each; (b) relationship between diameter of the most advanced (leading cohort) oocytes (*LC*) and mean value of all developing oocytes in wild, pre-spawning Barents Sea cod. 95% prediction bands are shown (95% confidence intervals were too tight to be illustrated). Note that a few females apparently were in final oocyte maturation (*FOM*) (*LC* > 800 μm) (Kjesbu, Kryvi, et al., 1996). *VP* refers to the (pre-spawning) vitellogenic period. The vertical bar denotes the separation between *VP* and *FOM*

LC > 250 μm, was set to typically begin on 8 October, that is including a latency period after autumn equinox (Kjesbu et al., 2010); cod starts maturing gonads for the upcoming spawning season when the night gets longer than the day (Davie et al., 2007; Kjesbu et al., 2010; Woodhead & Woodhead, 1965). Following estimation of the corresponding total length of this temperature-dependent, maturity (vitellogenic) period (*VP*, in days) (Kjesbu et al., 2010) (Table 2, Equation 5), the pre-spawning daily increase in vitellogenic oocyte dry weight, ΔVDW_P (in μg day^{-1}) could be indicated (Table 2, Equation 6). This

equation implied that VDW_{MOD} at LC = 250 μm, that is prior to any vitellogenin uptake, was considered negligible, indicated by extrapolation. Finally, the daily increase in dry weight for the entire vitellogenic mode, $\Delta VDW_{P_{overall}}$ (in g day^{-1}) could be established (Table 2, Equation 7).

The studies on **experimental females** of Barents Sea cod were approved by the Animal Welfare Committee (today within the Norwegian Food Safety Authority, www.mattilsynet.no) and conducted by licensed experimenters. The resulting exploratory analysis concentrated on data sets from the 2000, 2001 and 2002 'experimental season', as there were signs of a 'warm wave' (Appendix S1, List of Abbreviations and Terms) (as measured in the inlet water) in 2002, transient in 2001 but absent in 2000 (Figure 2). Including also related type of data from published experiments (see below), the ambient *T* ranged from 4 to 10°C, with the corresponding oxygen saturation level decreasing by 13.21% (32 psu salinity, 760 mm Hg) (https://water.usgs.gov/water-resources/software/DOTABLES/). The currently studied experimental females originated from a larger trawl sample taken in the southwestern (71° N 18–26° E) and central Barents Sea (74° N 19° E) in October 1999 (*N* = 72; spawning season 2000) and August 2000 (*N* = 350; spawning season 2001 and 2002), respectively. The whole catch was in each case transported to IMR facilities in Bergen, Norway, all specimens measured and PIT-tagged (using as always anaesthesia during all handling), and placed in two outdoor feeding tanks, each 30 m^3 (8–9°C; Dan-Ex 1562 dry pellets (www.biomar.com)). Their *TL* ranged from 50–60 cm, that is foreseen to become first-time (recruit) spawners in the following season (Marshall et al., 2006). As the reproductive cycle advanced nearer spawning, the sex was determined by stripping, or, if no egg or milt release could be detected, by inserting a soft, 2-mm thick plastic tube in the gonadal duct to remove a small piece of gonad tissue by suction ('catheterization') to be inspected microscopically (Kjesbu, Kryvi, & Norberg, 1996) but also, in the case of females, to predict time of start of spawning from the measured *LC* (Kjesbu et al., 2010). In effect, 'cod pairs' (pair = one female and male) (Brawn, 1962) were in January/February randomly selected by length-stratified sampling from the larger group of individuals in the feeding (storage) tanks and moved into each of 10 separate, 20 m^3 indoor spawning chambers in a 15-m diameter circular tank (8–10°C, simulated light cycle at 60° N) (Kjesbu, Solemdal, et al., 1996). Ovarian catheterization, typically three times per individual, was applied to track oocyte development (Kjesbu, Kryvi, & Norberg, 1996; Thorsen & Kjesbu, 2001). After spawning, each individual was processed, considering in the further data handling only those females (*N* = 24) confirmed by dissection to show no remaining developing oocytes in their ovarian tissue (Appendix S1, Table S1). On the route to contrast $\Delta VDW_{S'_{overall}}$ with $\Delta VDW_{P_{overall}}$, a further list of algorithms was constructed (Table 2) to calculate—for each female—(i) total oocyte (egg) dry weight just before any egg release (*TEDW_P*, in g, P = pre-spawning) (Table 2, Equation 8), (ii) realized total egg dry weight (*TEDW_{P+S}*, in g, S = spawning) (Table 2, Equation 9), (iii) the resulting increase in total egg dry weight attributed to the act of spawning as such (*TEDW_S*, in g), (Table 2, Equation 10), and finally, including

the length of the spawning period (SP, in days), (iv) $\Delta VDW_{S, \, overall}$ (in g day^{-1}) (Table 2, Equation 11). As above, these estimates were built on observed data sets (Appendix S1, Table S1).

In the further preparation for the below standardized model simulation, the three-season experiment was used to provide the number of batches spawned per female (N_B) as a function of the number of eggs spawned (realized fecundity; F_R, in millions) (Table 2, Equation 12). F_R fitted better ($r^2 = .592$, $p < .001$) as explanatory variable than W ($r^2 = .438$, $p < .001$) or TL ($r^2 = .388$, $p < .001$). The typical batch fecundity (F_B, in thousand) was thereafter set as a function of F_P and N_B (Table 2, Equation 13). This expression required that F_P could be taken as a proxy for F_R, which seemed reasonable (Figure 3a). The varying number of eggs per batch was accounted for in the estimation of the overall, weighted mean egg diameter (WEDIAM) and dry weight (WEDW) (Kjesbu, Solemdal, et al., 1996; Ouellet et al., 2001). WEDIAM and WEDW were highly related ($r^2 = .955$, $p < .001$). However, in contrast with expectations (Chambers & Leggett, 1996; Marteinsdottir & Steinarsson, 1998), the present dataset (Appendix S1, Table S1) provided no evidence for a relationship between WEDW and TL or W, or combinations of these body metrics ($p \geq .365$). We, therefore, decided to use the power function curve established for Norwegian Coastal cod South (hereafter Coastal cod South) (Appendix S1, List of Abbreviations and Terms) (Kjesbu, Solemdal, et al., 1996), supported by that this curve (Table 2, Equation 14) safely fell within the presently established 95% confidence band for Barents Sea cod.

To contrast $\Delta VDW_{P, overall}$ and $\Delta VDW_{S, overall}$ under, as far as possible, identical preconditions in the following calculation exercise, named for clarity the **model simulation** (Appendix S1, Table S2), TL was set to range from 50 to 105 cm, T held at 9°C and pre-spawning LC set at 800 μm. Consequently, LC = 800 μm functioned as a starting point for the subsequent oocyte growth during spawning ('single cohort') (Appendix S1, Table S2). As an alternative, oocyte growth was also set to start as early as at MOD ('averaged cohort'), copying in all other aspects the former calculations and, therefore, not dealt with further here (Table 2). However, an accurate calculation of the rate of incorporation of oocytic dry matter during spawning required first information on the spawning frequency (S_f, in h^{-1}) at T = 9°C, using in this respect the Q_{10} law (Kjesbu, 1989; Schmidt-Nielsen, 1983) (Table 2, Equation 15), to thereafter provide the resulting spawning interval (SI, in h) (Table 2, Equation 16). Following these parametrizations, the typical increase in single oocyte dry weight within each SI, that is ΔVDW_S (in μg day^{-1}), could be given (Table 2, Equation 17). As VDW_{LC} in Equation 17 refers to LC = 800 μm, ΔVDW_S should mimic the subsequent uptake during final oocyte maturation (FOM) (Kjesbu, Kryvi, & Norberg, 1996) (Figure 3b). Finally, the resulting cohort (batch) investment, $\Delta VDW_{S, \, overall}$ (in g day^{-1}), was given by multiplying with F_B (in thousand) (Table 2, Equation 18).

2.1.2 | Spawning frequency

Since the spawning frequency (S_f) of the present species is evidently influenced by ambient temperature (T), that is higher at warmer Ts

(Kjesbu, 1989), this reproductive trait was selected to pinpoint any related optimal (T_{opt}) and upper pejus temperature (T_{up}) during the act of spawning (see Introduction).

The analysed 19 **experimental females** (Table 1) showed at least a few fertilized eggs per batch. This further selection out of the above-studied 24 females (Table 1; Appendix S1, Table S1) was necessary to be able technically to collate complete observational series of S_f per female and season as a function of T. The length of the spawning interval (SI, in h)—the inverse value of S_f (see above)—formed the basis for this calculation exercise. SI was given from detailed egg developmental rates at the actual T (Kjesbu, 1989; Kjesbu, Solemdal, et al., 1996); T was measured daily just below the sea surface, where the eggs in each spawning chamber (see above) were floating. In some cases T was interpolated, as specified in Appendix S1 (Figure S2). This approximation was feasible due to the high stability in T from one day to the next (but not over the whole season as such; Figure 2), except for in 2002 in connection with the pulsed production of relatively warmer water (warm wave), requiring closer tracking of the day-to-day changes in T (Appendix S1, Figure S2). Data on Coastal cod South (Kjesbu, 1989)—13 females in indoor tanks and 2 females in cooler, outdoor tanks—were added to this S_f and body metrics dataset (Table 1). To further increase the analytic breadth, averaged SI per female—and thereby averaged S_f per female—were also extracted for Gulf of St Lawrence (GStL) cod, held at 2 ($N = 17$) to 4–5°C ($N = 21$) (Ouellet et al., 2001) (Table 1).

To locate any T_{up} from the complete, seasonal series on S_f as function of T for each of the above-mentioned 19 experimental females of Barents Sea cod (Appendix S1, Table S1), they were firstly ranked by increasing max. T. Any trends were further illustrated by clarifying which of these individuals experienced common temperature conditions ($N = 11$) and which ones experienced a warm wave ($N = 8$). The specific location of T_{up} was thereafter given by studying even more detailed tracking data, focusing on any abrupt irregularities in S_f versus T for each female (Appendix S1, Figure S2). This analysis also consulted information on aquaculture (broodstock) cod showing a statistically significant drop in the overall fertilization rate for $T > 9.6$ (van der Meeren & Ivannikov, 2006), and finally, supplemented with dst-based information (Appendix S1, List of Abbreviations and Terms) on spawning T from several cod stocks in the Northeast Atlantic. So, the adopted range (±0.25°C) in T_{up} resulted from carefully evaluating S_f dynamics vs. max T or T and literature information but also considering any likely uncertainty in the actual ambient T in the tank, though excluding any measurement error in T (given from an oceanographic thermometer).

2.1.3 | Embryos

To **experimentally** clarify to what extent ocean warming impacts early life-history stages, represented by embryos, MFERT (mean fertilization rate per batch, based on 100 eggs) and the associated MEDW (mean egg dry weight, see below) were linked to the encountered,

ambient T during single spawning intervals (Appendix S1, Figure S2). This aggregated analysis on 19 females was followed by in-depth tracking of $MEDW$ across the season for five females experiencing different maximum temperatures (Table 1), that is max. T reaching either 9.1 ($N = 2$) or 10.2–10.3°C ($N = 3$) (Appendix S1, Table S1). The latter category referred to those females, which showed an extended overlap between spawning activity and the appearance of the warm wave (7, 8 and 8 out of 17, 21 and 13 egg batches, respectively). To measure $MEDW$, a total of 50 eggs per batch were flushed with distilled water and completely dried prior to any weighing (Kjesbu, 1989; Kjesbu, Solemdal, et al., 1996). The associated batch fecundity was displayed (Appendix S1, Figure S3), given by entering the mean egg diameter (based on 50 eggs) in a packing density formula and multiplying with the total volume of eggs in that particular batch (Kjesbu, 1989).

2.2 | Climate impacts on cod spawning ground persistence

Observed and modelled environmental temperatures (Table 1) were used to indicate the consequences of exceeding the upper pejus temperature (T_{up}). The associated uncertainty in the resulting T_{up} (see Section 2.1.2) was implemented in a sensitivity analysis when assessing the implications for the likely fate of southern spawning grounds, that is in waters of likely, immediate interest. This research was supported by an in-depth review on 'Observed shifts in cod spawning grounds in the Northeast Atlantic' (Appendix S1).

2.2.1 | Observed trends in global and regional temperature

The dataset (HadSST.3.1.1.0) used to display the global trend in sea surface temperature (SST) anomalies (1850–2018) (Figure 1a) was downloaded from the Met Office Hadley Centre (www.metoffice.gov.uk/hadobs/hadsst3/data/download.html), with anomalies relative to the average for 1961–1990 (Rayner et al., 2006). For the Barents Sea, the presented annual and 5-year smoothed temperature refer to the Kola Transect (70°30′–72°30′ N, 33°30′ E, 0-200 m, 1900–2018) (Boitsov et al., 2012) (Figure 1b). For the North Sea, this hydrographic information originated from the Hanstholm—Aberdeen (57° N)—Utsira (59°20′ N) Transect (0–100 m, 1958–2008), running ROMS_AA10km_CORE2 (see below).

2.2.2 | Fate of southern cod spawning grounds

The Regional Ocean Model System (ROMS) (Shchepetkin & McWilliams, 2005) was first run as a hindcast simulation for the recent decades with atmospheric forcing from the Coordinated Ocean Research Experiment CORE2 reanalysis 1958–2007 (Large & Yeager, 2009) and lateral boundary conditions from the Simple Ocean

Data Assimilation (SODA) dataset (Carton & Giese, 2008) (Table 1). Thereafter, the model was initialized and forced with output from the coupled Norwegian Earth System model NorESM1-M (Bentsen et al., 2013) for the Representative Concentration Pathway RCP4.5 scenario from 2006 to 2070 (Table 1). The model domain covers the North Atlantic-Arctic Ocean with an average resolution of about 10 km (i.e., AA10km grid, where AA = Atlantic-Arctic) in the Nordic and Barents Seas. Further details of the model setup and corresponding model evaluation are described in recent literature (Sandø et al., 2021).

Based on timeseries of observed and simulated temperature variability, two periods, 1965–70 and 2003–08, were chosen to represent cold and warm periods in recent decades, respectively (Sandø et al., 2020, 2021). Spawning T for cod were taken from the bottom layer in the case where the depth is less than 100 m, and at 100 m where the bathymetry is even deeper. The projection of the 2060s was based on a downscaling of one ensemble member from the NorESM-1 M RCP4.5 to be compared to the beginning of the same simulation, that is the 2010s, to minimize model biases. Within this scenario, suitable locations of cod spawning grounds in the southern distribution area were investigated with regard to T_{up}.

2.3 | Larval prey and recruitment proxies for North Sea cod

This section firstly considered the whole North Sea and thereafter focused on southern, northwestern and northeastern subareas (further specified below) to acknowledge the likely existence of subpopulations of North Sea cod (Holmes et al., 2014; Wright et al., 2018, 2021) to investigate links between copepod (cod larval prey) biography and cod recruitment dynamics at varying spatial (and temporal) scales (Table 1).

2.3.1 | Variation in copepod abundance in the North Sea

The Continuous Plankton Recorder (CPR) datasets at https://doi.org/10.17031/1758 ('Calanus') and https://doi.org/10.17031/1829 ('Small copepods')—provided by the CPR Survey at the Marine Biological Association of the United Kingdom, Plymouth, UK (https://www.cprsurvey.org/)—contained standardized abundances on *Calanus finmarchicus* CV-CVI, *C.* spp. stage CI-CIV, *C. helgolandicus* and *Para-Pseudocalanus* spp. The datasets were confined within the geographical area of 49.5 to 62° N and –4 to 10° E and spanned the period from 1958 to 2017 for the months of April to August. The CPR survey is undertaken by ferry boats and merchant ships ('ships-of-opportunity') that tow a plankton recorder in a fixed transect of the upper layer with a temporal resolution of about 1 month. Around 3 m^3 of water is sampled over the course of 10 nautical miles, which constitutes one unique CPR sample. Further details on the CPR survey are found in the published literature (Richardson et al., 2006), while the visualizations and analyses of the current study are specified in **Section 2.5**.

2.3.2 | Variation in copepod abundance in North Sea subareas

The abundances of the above-mentioned copepod categories were considered per North Sea subarea to be related to the performance (as specified below) of local populations of North Sea cod. So, for the copepod spp. time series to be directly comparable, we adopted the ICES division into subarea Southern (S), Northwestern (NW) and Viking4a (V4a, the adjacent Viking 20 in the Skagerrak was omitted) (ICES, 2017).

2.3.3 | Spawning stock biomass and recruits in the North Sea and subareas

An individual North Sea cod was set to reach sexual maturity at age 3 years (Nash et al., 2010). Hence, spawning stock biomass (SSB) forward lagged by 3 years (y + 3), SSB_yp3, was used as proxy for recruitment strength and related to the above-mentioned four category series on copepods (y). This correlation matrix was thereafter broadened by replacing SSB_yp3 with Recruitment (y + 1), that is Recruitment_y1. These cod stock metrics were extracted from ICES (ICES, 2015). Likewise, all current statements on stock-specific status refer to ICES (www.ices.dk). Next, SST was successively related with the abundance of C. finmarchicus, C. helgolandicus, Para-Pseudocalanus spp., as well as with North Sea cod SSB. North Sea SST per month (1958–2020) was downloaded from NOAA, USA (Huang et al., 2017) and then calculating the annual average. North Sea transect temperature (0–100 m) (1958–2008) at 57° N and 59°20′ (www.imr.no) (Figure 1c) was added for further insight (see above). This Hanstholm—Aberdeen—Utsira Transect is covered several times per year but to match as far as possible the spawning time of North Sea cod (January–April) (Brander, 2005), we selected T data from the month of March.

In the subarea-resolved analysis, cod population metrics originating from the international bottom trawl survey (IBTS Q1 and Q3) were used. This dataset provided subarea-specific indices on SSBs (SSB_yp3_NW, SSB_yp3_S and SSB_yp3_V4a) and recruits (Recruitment_y1_NW, Recruitment_y1_S and Recruitment_y1_V4a) back to 1983 (ICES, 2017), here further extended back to 1978 (co-author Peter J. Wright). Hence, this 'fine-scale zooplankton vs. cod analysis' spanned from 1978 to 2017.

2.4 | Spawning migration dynamics of Barents Sea cod

This exercise sought to quantify to which extent the degree the migration dynamics of Barents Sea cod has changed over recent decades, as measured by the directional displacement distance (D_D) and speed (U_D), split by body size category.

2.4.1 | Centre of gravity

These data derived from the 'Joint Norwegian-Russian Winter Survey' (February–March, 1981–2017) and the 'Joint Norwegian-Russian Ecosystem Survey' (August–September, 2004–2017), both surveys are detailed elsewhere (Jakobsen et al., 1997; Michalsen et al., 2011) (Table 1). The currently estimated centre of distribution (gravity) (CoG) averaged the number of cod per square nautical mile from standardized bottom trawl catches (Table 1). Latitude and longitude for each observation (catch) were converted into Cartesian coordinates. These computations in MATLAB R2016b resulted in the weighted average of CoG for small (30–59 cm in TL) and large cod (70–99 cm in TL), assumed to be sexually immature and mature, respectively. Individuals in the 60–69 cm size class were left out in order to keep these two maturation categories separate (Nash et al., 2010).

Only CTD stations taken in the vicinity of CoG were considered (Table 1), specified as ±0.5° in a latitudinal direction and ± 1° in a longitudinal direction. This grid design reflected the larger span in longitude (20–50° E) than latitude (71–77.5° N). The habitat depth was set at 100–150 m (Godø & Michalsen, 2000). Between 1981 and 1994 the CTD recorded every 5 m, from 1995 onwards every 1 m. The resulting number of CTD stations (1–17) per grid were, with few exceptions, higher during winter, typically 5, than during summer, typically 2–3. The grand mean across CTD stations within each grid was labelled as in situ (ambient) T (±SD). To compare with measures of environmental temperature, T in the Kola Transect (hereafter Kola T) (Figure 1b) in February, March, August and September were considered (Table 1). As winter CoG were 5-year smoothed, the same type of calculation exercise was applied on the four monthly resolved Kola T data sets (leaving the last 4 years unsmoothed).

2.4.2 | Displacement distance and directional speed

To better understand variation in D_D and U_D of large and small specimens over time, Kola T (see above), ice extent, SFA (suitable feeding area) and TSB (total stock biomass) were considered as 'drivers' (see the various time windows below) (Table 1). As the first step in this investigation, the ice extent was downloaded for the month of September (referring to the lowest values) (https://www.mosj.no/en/climate/ocean/sea-ice-extent-barents-sea-fram-strait.html), the SFA series (bottom T > 0°C, 72–80° N, 20–50° E) (Kjesbu et al., 2014) updated with more recent figures (Randi B. Ingvaldsen, IMR), and the TSB series extracted from a recent assessment report (ICES, 2020). D_D referred to the distance between the CoG in summer and the corresponding CoG in the following winter. For the larger cod this route reflected spawning migration (Sundby & Nakken, 2008). The distance between these two points was transferred to kilometres, accounting for Earth curvature (https://www.geeksforgeeks.org/

program-distance-two-points-earth/). The time in question (149–198 days) was given from logbooks, followed by calculation of U_D (m sec^{-1}).

2.5 | Additional data handling and statistical analyses

With reference to **Section 2.1** (cod physiology) and **Section 2.4** (Barents Sea cod migration), Systat 13 was used as the primary statistical software, that is eventually also SigmaPlot 14 in connection with publishable graphics (Inpixon, 2022). So, the given linear or power function regressions (Table 2) were from these packages. S_f and *MFERT*, being proportions, underwent arcsine transformation (Sokal & Rohlf, 1981) prior to parametric testing (two-sample Student *t*-test). The resulting probabilities were rechecked by running the non-parametric Kolmogorov–Smirnov test in parallel, finding irrelevant differences in *p*-values. The standard significance level at $p = .05$ was Bonferroni adjusted in cases of multiple Pearson correlation tests (Figure 12c). ArcGIS Desktop 10.8.1 was used for geographical positioning of *CoG*.

With reference to **Section 2.3.1** (North Sea copepod abundance) and **Section 2.3.2** (North Sea copepod abundance in subareas), all visualization and analysis of the CPR data were performed using R (R Core Team, 2019) and various libraries. For the ocean-basin decadal visualization, all unique samples were assigned to the correct ICES statistical rectangle (www.ices.dk) based on recorded longitude and latitude for each sample using the 'mapplots' library (Gerritsen, 2018). To avoid analytic bias caused by single or few observations, only ICES grid cells (0.5° Latitude × 1.0 Longitude) with 5 or more observations per decade were used. All abundance data were ln +1 transformed. To ensure all years and months within one decade were weighted equally, independent of variations in temporal and spatial sampling effort, the mean abundance of each copepod category was first calculated based on grid cell, month, year and decade, then on grid cell, year and decade and finally on grid cell and decade. This aggregated dataset was then further used as input to perform surface interpolation ('automap' library) (Hiemstra et al., 2009). Each interpolation was limited to the area confined by drawing a polygon around the outmost valid observations, which resulted in different decadal spatial distributions. In the subsequent subarea examination (i.e. by subarea S, NW and V4a)—to ensure observations being temporally and spatially comparable over the whole time series—only data occurring within unique ICES grid cells that contained at least 2 observations in the period April–August, as well as being sampled over at least 20 years, were considered.

With reference to **Section 2.3.3** (North Sea cod recruitment), illustrations and correlation statistics (Spearman) were consistently made with the ggscatter function from the R ggpubr library (Kassambara, 2020). The R function 'loess' was used to fit subarea specific time series curves.

3 | RESULTS

3.1 | Cod reproductive physiology

3.1.1 | Vitellogenin uptake

The power function (with *b* as exponent) for field-caught, experimental Barents Sea cod revealed a strong, positive effect of *TL* on the overall rate of oocytic dry weight (≈vitellogenin) uptake during spawning ($\Delta VDW_{S'overall}$) ($r^2 = .60$, $p < .001$, $b = 4.82$ (SE $= \pm 0.90$)) (Figure 4a). An allometric effect was also noticed for pre-spawning fecundity as such ($b = 3.59$ (SE $= \pm 0.09$)) (Figure 3a). $\Delta VDW_{P overall}$, supporting ovary growth prior to spawning (cf. pre-spawning reference curve), approximately equalled the modelled investment underlying the production of an egg batch (cf. single cohort) from final oocyte maturation (*FOM*) onwards (Figure 4a). However, apparently, two oocyte cohorts develop in succession (cf. averaged cohort) (Figure 4a). Thus, the next oocyte cohort quickly replaces the one entering *FOM* to be thereafter ovulated and released as eggs. Our modelled $\Delta VDW_{S'overall}$ in large females (*TL* > 70 cm) were obvious underestimates (Figure 4a), despite assuming a positive effect of body size on egg dry weight (Table 2, Equation 14).

3.1.2 | Spawning frequency

Although the steepness of the ascending spawning frequency (S_f) curve was modest within increasing T (≈4 < T < ≈9°C), the variation in spawning interval length (*SI*) ($p < .01$)—and thereby in S_f (Figure 4b; Figure 5, Appendix S1, Figure S1)—suddenly turned markedly higher above this thermal window (Figure 6a,b), though not statistically departing from the general *SI* level as such ($p = .31$) (Figure 6c). Arbitrarily changing Q_{10} from 2 to 3 hardly had any impact on modelled S_f (Figure 4b). No clear indications of differences in S_f existed between the two cod stocks presently addressed, Barents Sea cod and Coastal cod South (Figure 4b). The inclusion of averaged S_f for Gulf of St Lawrence (GStL) cod fell into this depiction at 2°C but only marginally at 4–5°C, but neither S_f ($p = .21$) nor pre-spawning body condition changed significantly ($p = .27$) between these two temperature regimes (Figure 4b), consulting tabled data (Ouellet et al., 2001). As for GStL cod ($p > .05$), mean S_f for Barents Sea cod were unaffected by pre-spawning body size (*TL*: $p = .46$, *W*: $p = .32$, $8.5 < T_{mean} < 9.1$°C, $N = 11$). In the latter case, the more detailed picture showed that $T ≥ 9.6$ (± 0.25)°C, even brief in nature, caused the normally highly rhythmic ovulatory cycle to turn erratic and remain so even if T thereafter decreased (Figure 5; Appendix S1, Figure S2). This adopted uncertainty in T_{up} (Figure 5) was included in the subsequent field-related sensitivity analysis in **Section 3.2.1**.

3.1.3 | Embryos

The phenomenon of warm waves (Figure 2) did not statistically influence the subsequent mean fertilization rate of single egg batches (*MFERT*) ($p = .53$), though *MFERT* generally fell by a few percent
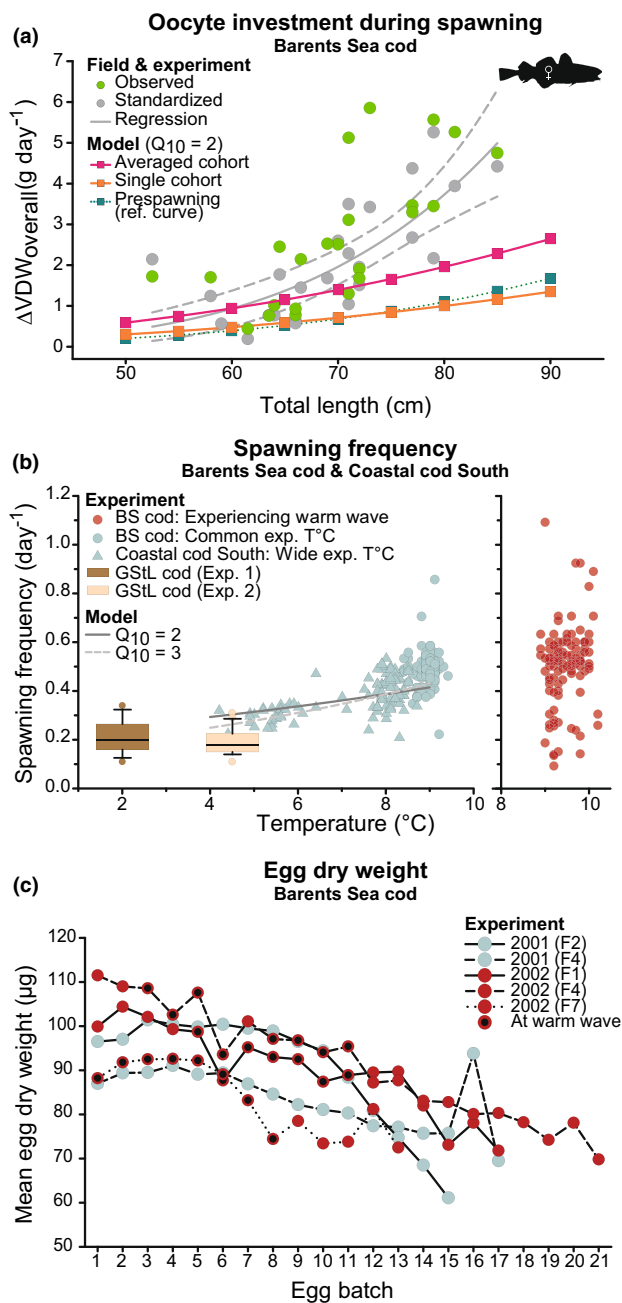
FIGURE 4 Cod reproductive physiology and spawning performance. (a) Observed and modelled typical daily rate of oocytic dry weight (≈vitellogenin) uptake ($\Delta VDW_{overall}$) at 9°C of Barents Sea cod in relation to total length. The field-experimental data curve (mean ± 95% confidence interval) was standardized by maturity phase (leading cohort = 800 μm) at initiation of spawning. In the model simulation ($Q_{10} = 2$) three calculation paths were followed: pre-spawning, single and averaged oocyte cohort production, assuming in the latter two cases that the mean egg dry weight of a single batch increases with body size; (b) spawning frequency (S_f) regressed on the corresponding temperature (T) of experimental Barents Sea cod and coastal cod south, categorized by T regime—'warm wave', 'common' or 'wide'—where 'warm wave' (see main text) being further subdivided into 'at and after this event'. The earlier published $Q_{10} = 2$ (Kjesbu, 1989) was supplemented by $Q_{10} = 3$ to model the subsequent response in S_f. Published mean S_f data for Gulf of St Lawrence (GStL) cod (Ouellet et al., 2001) at 2 and 4–5°C were added for further contrast; and (c) trend in single batch mean egg dry weight during the spawning period (from first to last egg batch) of five experimental Barents Sea cod, where three of them encountered incidences of $T \geq 9.6°C$ (Appendix S1, Table S1)

farther north in the Irish Sea (Figure 7a,b; Appendix S1, Observed shifts in cod spawning grounds in the Northeast Atlantic). The southernmost spawning grounds seemingly dissipated in conjunction with the northward expansion of the 9.6°C isotherm (T_{up}, see above) (Figure 7a,b). The inclusion of an uncertainty of ±0.25°C in the assessment of this threshold (Figure 5), resulted in a broadening of this boundary zone (Figure 7a,b). However, this sensitivity test showed markedly larger bands west of Ireland, that is an area lacking cod spawning grounds (Figure 7a,b). Our following projection pointed to extirpation of the spawning grounds in the Celtic Sea (and the adjacent Bristol Channel) and English Channel within a few decades (Figure 7a–c). The existence of spawning grounds in the Irish Sea was also apparently at risk (Figure 7a–c).

3.3 | Larval prey and recruitment proxies for North Sea cod

Except for farthest south in the North Sea, T in this ocean basin will most likely remain below T_{up} at cod spawning grounds in the next half-century (Figure 7c). Historically, cod spawning appeared throughout most of the North Sea (Appendix S1, Observed shifts in cod spawning grounds in the Northeast Atlantic) but is today increasingly confined to the Northeast subarea, that is in ICES Viking4a (Figure 7b).

3.3.1 | Whole North Sea

C. finmarchicus and *C. helgolandicus* evidently responded oppositely to environmental temperature, represented by *SST* (Figure 8a,b). Their decadal and multidecadal shifts in distributional abundance were also distinctly different (Figure 9a,b). Although an insignificant trend was seen for *Para-Pseudocalanus* spp. versus *SST* (Figure 8c), its presence in the North Sea was

points (Figure 6d). The corresponding, generally longer spawning interval (*SI*) (Figure 6a) lowered *MFERT* ($p \leq .03$) in two out of eight cases; six females exhibited no such relationship ($p \geq .32$) (Figure 6e). There was no sign of that a warm wave affected mean egg dry weight (Figure 4c) or batch fecundity (Appendix S1, Figure S3).

3.2 | Climate impacts on cod spawning ground persistence

3.2.1 | Fate of southern cod spawning grounds

Over the period from the cold 1960s to the warm 2000s, cod egg concentrations in the Irish/Celtic Sea-English Channel Complex undoubtedly declined, though dense aggregations were still seen
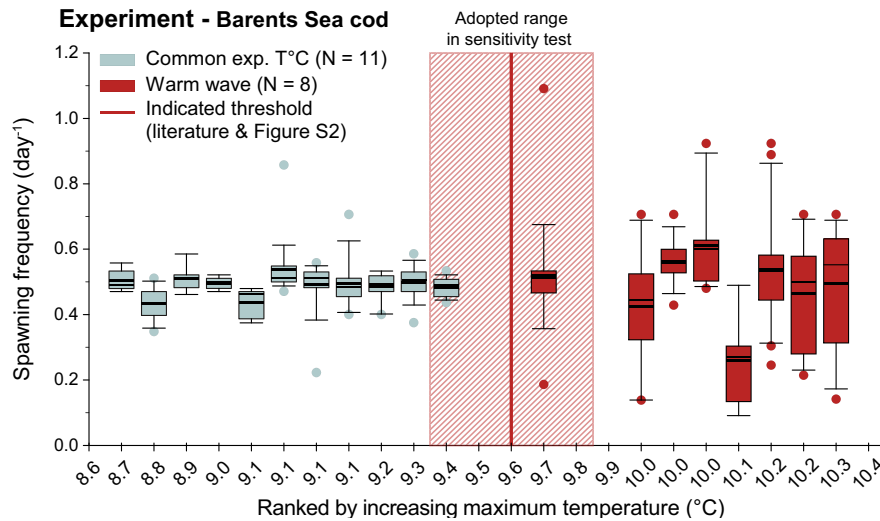
FIGURE 5 Detailing the spawning frequency of individual females of Barents Sea cod (Appendix S1, Figure S1 and Table S1) in relation to the maximum temperature encountered during the spawning period. The females were split into those experiencing common temperature conditions in the laboratory and those experiencing a warm wave, the latter as defined in Appendix S1 List of abbreviations and terms. Box plot: 10th (whisker), 25th (box), 75th (box) and 90th percentile (whisker), mean (thick line) (box) and median (thin line) (box), and outliers (symbol); line at 9.6°C: the foreseen upper pejus temperature (T_{up}); shaded rectangle: the adopted range (±0.25°C) in T_{up}

generally diminishing (Figure 9c), as for *C. finmarchicus* (Figure 9a). The corresponding North Sea cod *SSB* vs. *SST* relationship was clearly negative (Figure 8d). As for *SST* (1958–2020), *T* in central and northern North Sea transects (0–100m, 1958–2008) fluctuated in an approximate cyclic, decadal manner but since 2000 showing a more-or-less steady increase (Figure 1c).

SSB_yp3 and *Recruitment_yp1* of North Sea cod were positively correlated with *C. finmarchicus* as well as with *C.* spp. (CI-CIV) abundance ($p<.001$), whereas negatively with *C. helgolandicus* abundance ($p<.001$) (1960–2017; Appendix S1, Table S3). *Para-Pseudocalanus* spp. and *SSB_yp3* ($p = .01$) related positively but no such likely effect could be seen for *Recruitment_yp1* ($p = .07$) (1960–2017; Appendix S1, Table S3). North Sea cod *SSB_yp3* largely mirrored *C. finmarchicus* abundance; our extension (1999–2017) of the earlier 39-year time series (1960–1998) by Beaugrand et al. (2003) (Appendix S1, Table S4) showed a joint switch to increasing trends in the late 1990s (Figure 10a), though all these more recent data points were far below earlier values, that is located near the origin of this regression (Figure 10b).

3.3.2 | North Sea subareas

There was a clear variability in copepod abundance across North Sea subareas (statistical rectangles) (1958–2017) (Figure 11a,b). The presence of *C. finmarchicus* in the Northwestern (NW) subarea markedly declined from 1958 but with indication of a partial recovery since the mid-1990s (Figure 11b). *C.* spp. (CI-CIV) and *Para-Pseudocalanus* spp. exhibited very much the same pattern as *C. finmarchicus* (Figure 11b). In the Southern (S) subarea a more persistent declining trend was noticed for each of these three copepod categories but likely flattening out in the case of *C. finmarchicus* since

the 2000s (Figure 11b). The process of data quality assurance led to instances of omitted grid cells, particularly in Viking4a (V4a) subarea (Figure 11a). However, *C. finmarchicus* also in this subarea underwent a decline in abundance but with recent signs of recovery, as in the NW subarea (Figure 11b). Here as well, *C.* spp. (CI-CIV) largely reflected *C. finmarchicus* patterns while *Para-Pseudocalanus* spp.—after a decline—showed indication of a slight recovery but then stagnation from the 1980s (Figure 11b). *C. helgolandicus* in NW and V4a subareas is obviously on a rise whereas exhibiting a rather stable level in S subarea (Figure 11b). Finally, except for *Para-Pseudocalanus* spp., the abundance as such within each copepod category noticeably increased from S, via NW to V4a subarea (Figure 11b). However, these separate clines referred to different orders of magnitude, with *Para-Pseudocalanus* spp. most numerous (Figure 9; Figure 11b).

The consulted IBTS indices (1978–2017) clarified that the important role of the S subarea in upholding North Sea cod productivity is diminishing (Figure 11c). *SSB_yp3_S* and/or *Recruitment_yp1_S* evidently related positively to *C. finmarchicus*, *C.* spp. (CI-CIV) and *Para-Pseudocalanus* spp. abundances, but negatively so for *C. helgolandicus* (Appendix S1, Table S5). For the NW and V4a subareas, these types of correlations were highly mixed in nature (Appendix S1, Table S5), accompanied by rather stable *Recruitment_yp1_NW* and *Recruitment_yp1_V4a* but recently increasing *SSB_yp3_NW* and *SSB_yp3_V4a* (Figure 11c).

3.4 | Spawning migration dynamics of Barents Sea cod

The considered drivers displayed large temporal dynamics within the current migration study (2004–2017) (Figure 12a, Appendix S1, Figure S4, Table S6). Both summer and winter in situ (ambient) *T*
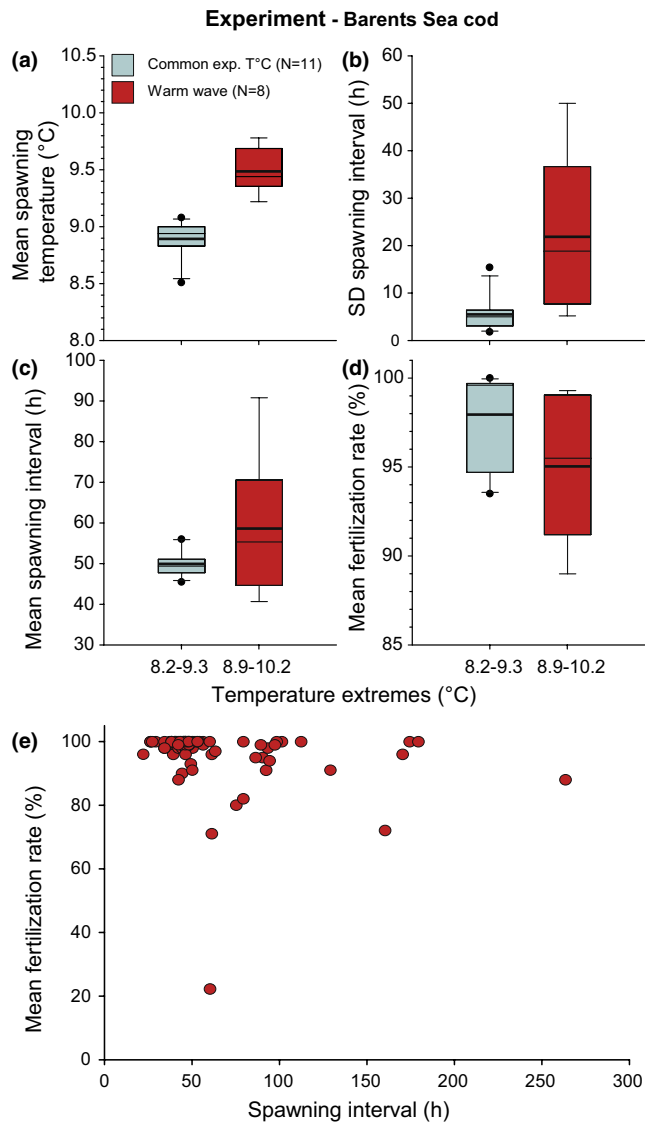
FIGURE 6 Aggregated information on variation in spawning performance for captive Barents Sea cod, grouped by ambient temperature regime, either $8.2 < T < 9.3$, or $8.9 < T < 10.2°C$: (a) mean spawning temperature; (b) standard deviation (SD) of spawning interval; (c) mean spawning interval; (d) mean fertilization rate per batch; and (e) mean fertilization rate as a function of spawning interval. Panels (a) to (d) display 10th (whisker), 25th (box), 75th (box) and 90th percentile (whisker), grand mean (thick line) (box) and grand median (thin line) (box) and outliers (symbol). Same material and definition of common and warm wave as in Figure 5

position between summer and winter (Figure 12b). However, large specimens could also migrate farthest north during summer (Figure 12b). Our correlation coefficient flowchart spoke for an indirect effect of ocean warming (*Kola T*), cascading—in combination with the reduced ice extent—to an enlarged suitable feeding area (*SFA*) followed by an improved total stock biomass (*TSB*) and then to a pronounced increase in both Barents Sea cod displacement distance (D_D) and directional speed (U_D) (Figure 12c). On the contrary, the direct effect of *Kola T* explained only about 4% and <1% of the deviance in D_D in small and large cod, respectively (Figure 12d). For the latter group of individuals—the subsequent spawners—*TSB* explained 75% of the deviance in D_D (Figure 12e) and 65% for U_D (Figure 12f).

4 | DISCUSSION

We believe that the approach and methodology used in this study on Atlantic cod might serve as a template for future studies exploring thermal limitations of teleost reproduction. Our investigation on the life history and reproductive ecology of the cold-temperate *G. morhua* reveals that local persistence under climate change is constrained by (1) knife-edge ovulation requirements, (2) altered larval prey biogeography and (3) energetically costlier spawning migrations, illustrated by the Irish/Celtic Seas-English Channel Complex, North Sea and Barents Sea scenario, respectively. Hence, each of these three addressed causal mechanisms is highly habitat specific. Obviously, a series of other stressors are involved too, such as harvest rate (Hutchings, 2000) and lower trophic level productivity due to strengthened stratification (at least in the southern domain addressed here) (IPCC, 2021), but the performance of the currently addressed traits are fundamental for continued stock persistence. So, this article complements related studies that either address consequences of one single stressor, as seen in meta-analyses (Dahlke et al., 2020; Free et al., 2019), or, on the other end of the scale, undertakes expert scorings of multiple stressors for both data-poor and data-rich stocks (Hare et al., 2016; Kjesbu et al., 2022). The current line of research asked for access to vast, in-depth biophysical information, where Atlantic cod was the logical choice as study subject.

To circumvent the overriding investigative problem attributed to 'extremely scarce' reproductive data for teleosts in general, and especially in view of ocean warming (Dahlke et al., 2020), we addressed relevant, basic reproductive physiology aspects of Atlantic cod as an example, given that this is a relatively well-studied species. The resulting experimentally observed, spawning frequency (S_f) data clearly did not fit into the conventional thermal performance curve (Levesque & Marshall, 2021). The key deviation was the presence of both high and low S_f for a given individual past a rather moderate T, here defined as T_{up}, corresponding to 9.6 (±0.25)°C. Rightly so, there might be 'cells of water' in each of the 20-m^3 spawning chamber differing in T from the presently recorded surface T implying that the ambient T—leading to T_{up}—might be partly biased, though it should

undulated in partial synchrony with *Kola T* (Appendix S1, Figure S4). However, *Kola T* inadequately reflected the encountered hydrographical conditions as such; ambient T during winter was significantly higher, except for small cod in recent times (Appendix S1, Figure S4a), and conversely, significantly lower during summer (Appendix S1, Figure S4b).

Most centre of gravities (*CoGs*) fell within a southwest-northeast 'route' in the Barents Sea, with markedly higher variation in summer than in winter (Figure 12b). Large and small cod swapped latitudinal
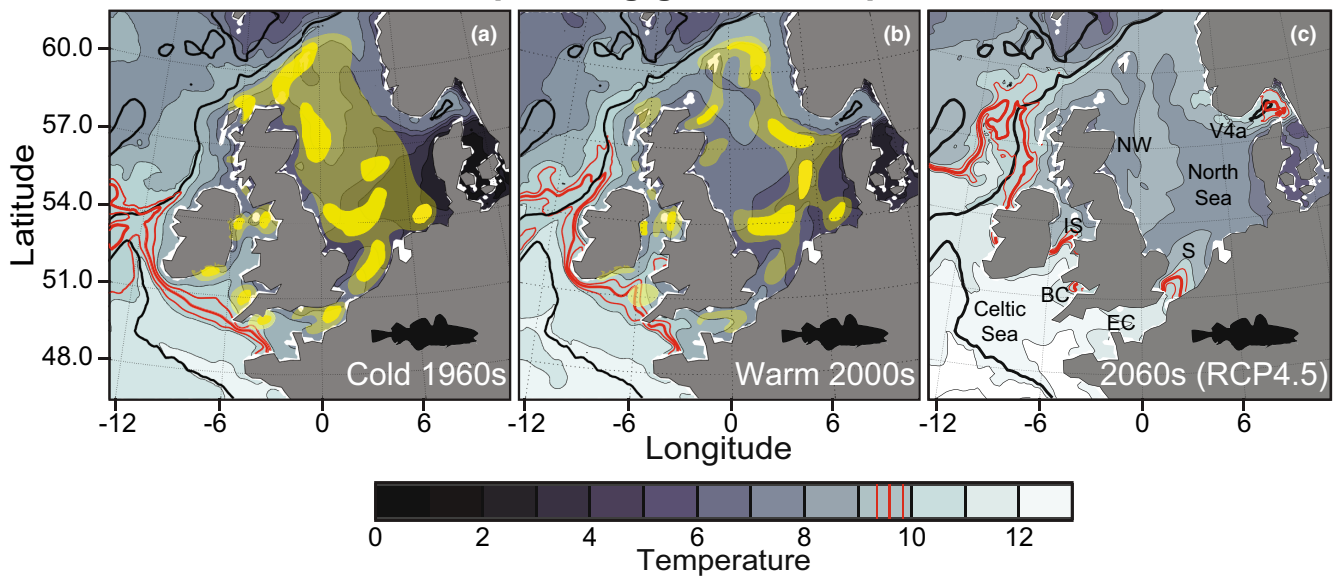
Cod spawning grounds displacement

FIGURE 7 Observed shifts in cod spawning grounds in the Irish/Celtic Seas-English Channel complex and North Sea in the cold 1960s and warm 2000s and the projected southern border for suitable cod spawning in this region in the 2060s. (a) Downscaled hindcast simulations (ROMS—CORE2) of bottom temperature (March) in the cold 1960s and (b) warm 2000s and (c) forecast simulations (ROMS—NorESM-RCP4.5) to 2060, with the $9.6 \pm 0.25°C$ (thick and thin red line, respectively) isotherm (T_{up}) annotated in all three panels. BC = Bristol Channel, EC = English Channel, IS = Irish Sea, NW = northwestern subarea, S = southern subarea and V4a = Viking 4a (northeastern) subarea. (a), (b) and (c) are provided with 1°C-resolved isotherms (thin black lines) and the 500-m isobath (thick black line). The specific location of spawning grounds (yellow colour) in (a) and (b) was the result of dedicated reviews (Appendix S1, Observed shifts in cod spawning grounds in the Northeast Atlantic).

be kept in mind that cod swim upwards in the water column during courtship behaviour (Brawn, 1962). Much more important—and validated by field observations—is that the existence of a knife-edge threshold during spawning is strongly supported by data storage tag (dst) information (Appendix S1, List of Abbreviations and Terms) from a series of North Atlantic cod stocks (Righton et al., 2010). However, the illustrated data in Righton et al. (2010) do not allow for precisely pinpointing any T_{up}, except for that this threshold is found somewhere between 8 and 10°C. Nonetheless, the Gulf of St Lawrence cod (Ouellet et al., 2001) showed indications of offset, lower S_f values already at 4–5°C, which probably relates to this stock being adapted to spawn at extraordinarily low temperatures, that is around 0°C (Brander, 2005). So, there is seemingly a degree of plasticity at lower temperatures in acclimatized stocks but whether this might happen in warmed waters is yet uncertain. The notion that any optimal temperature (T_{opt})—mathematically defined as $dS_f/dT = 0$—was non-existent questions the predictive value of the oxygen- and capacity-limited thermal tolerance (OCLTT) theory (Pörtner et al., 2017; Pörtner & Farrell, 2008) in an transient setting such as ovulation, in line with related physiological arguments (Jutfelt et al., 2018). This lack of T_{opt} should explain why spawning ground temperatures across cod stocks in the North Atlantic are not constant (Brander, 2005). Moreover, the seemingly inflexibility in T_{up}, coupled with that erratic S_f persisted after T decreased, challenges any practise of extrapolating generally accepted principles within aerobic scope theory to this specific part of reproductive

physiology. Yet, it is unknown if this observed unstable S_f pattern down to presently 8.9°C is maintained if T continues to decrease.

Although the proximate physiological cause behind this likely non-adaptive T_{up} remains unknown, the 'weak link' is likely found within the extensive list of potential endocrine or enzymatic factors obstructing ovulation at $T \geq T_{up}$ (Alix et al., 2020). According to aquaculture cod broodstock studies the overall fertilization rate in tanks significantly drops at $T > 9.6°C$ (van der Meeren & Ivannikov, 2006). We were unable to demonstrate this negative effect statistically on single egg batches (*MFERT*); our experiment focused on individuals with at least some fertilized eggs in each batch in order to be able to calculate S_f from the T-dependent egg development rate. However, the circumstance that *MFERT* often did not noticeably fall following exceedingly long spawning intervals (low S_f) indicates that these advanced oocytes still remained in their supporting follicles instead of being ovulated and retained in the ovarian lumen under accumulating shortage of oxygen, cf. the 'egg-bound syndrome' (Hansen et al., 2016). The resulting egg size, represented by *MEDW*, is in cod determined by a sharp surge in vitellogenin during final oocyte maturation (Kjesbu, Kryvi, & Norberg, 1996). Warm waves (Figure 2) apparently did not disturb this route of vitellogenic sequestration (Alix et al., 2020; Kjesbu et al., 1991; Servili et al., 2020; Tyler & Sumpter, 1996). Likewise, no effect could be detected on batch fecundity, which seems reasonable as the fecundity of *G. morhua* is principally settled ahead of spawning (Kjesbu et al., 1998). One should, however, expect that the overall rate of vitellogenin uptake
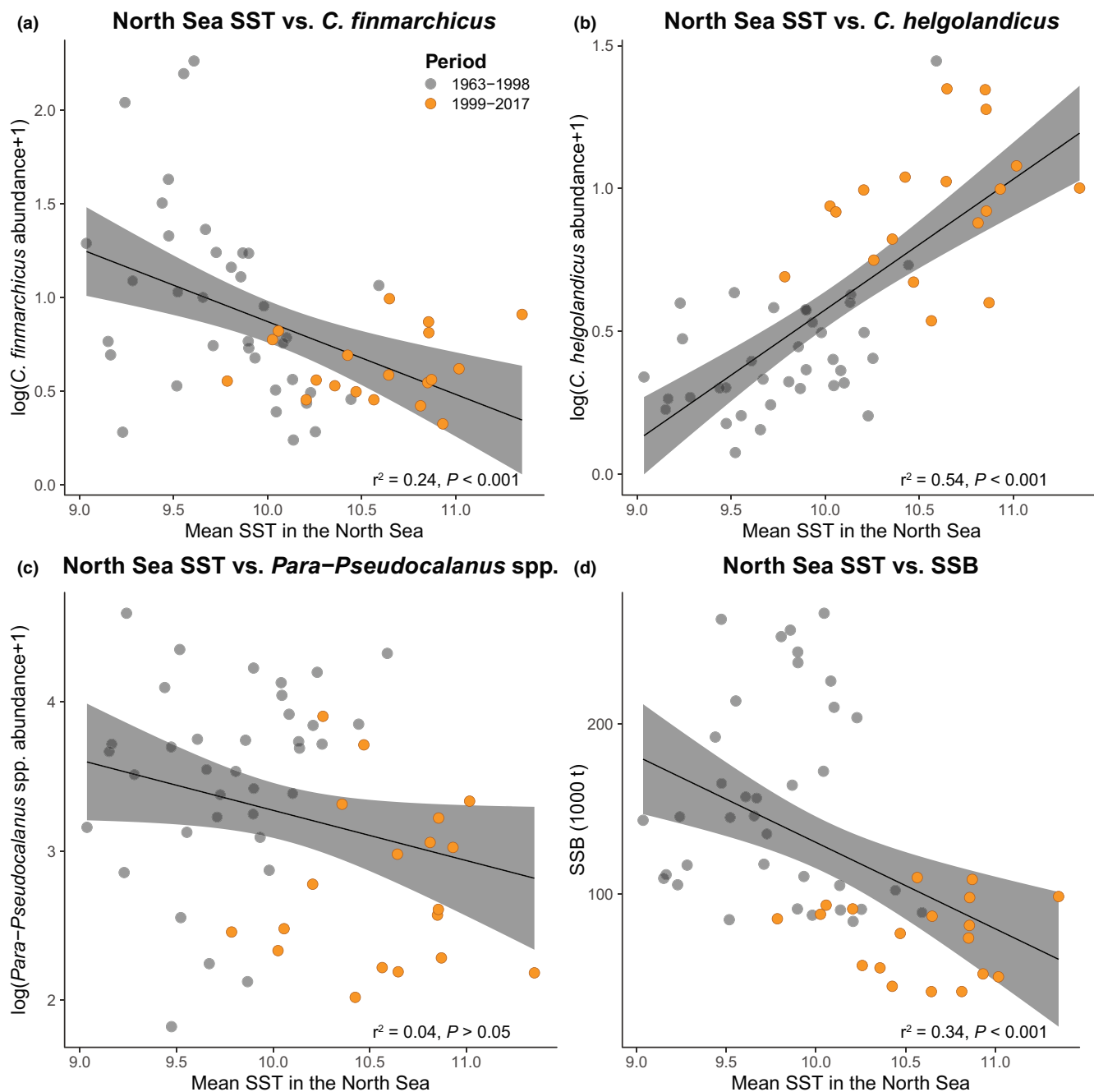
FIGURE 8 Long-term relationships (1963–2017) between sea surface temperature (*SST*) and *Calanus finmarchicus*, *C. helgolandicus*, *Para-Pseudocalanus* spp. and cod spawning stock biomass (*SSB*) in the North Sea. (a) *Calanus finmarchicus* abundance vs. *SST*; (b) *C. helgolandicus* abundance vs. *SST*; (c) *Para-Pseudocalanus* spp. vs. *SST*; and (d) North Sea cod *SSB* vs. *SST*. *SSB* is 3-year lagged. A linear regression line with 95% confidence intervals and the associated explanatory power are provided for each panel. The split into two subperiods refers to previous (Beaugrand et al., 2003) and currently extended analyses.

($\Delta VDW_{overall}$) would fall if a persistently high T is introduced prior to spawning due to the foreseen reduction in 17β-estradiol in several species (Alix et al., 2020). Anyhow, our formulations confirmed that the teleost ovulatory cycle is highly complex in nature (Charitonidou et al., 2022); in cod probably at least two oocyte cohorts co-develop. The further process of validation of $\Delta VDW_{overall}$ showed, however, clear examples of underestimates for larger individuals, suggesting that a much bigger share of the vitellogenic raw material is stored in muscle and liver in larger than smaller females (Jansen et al., 2021;

Kjesbu et al., 1991). In other words, ascribed to the usual pattern of (hyper)allometric reproductive investment in teleosts (Barneche et al., 2018). Hence, collectively, gonad size as such does not fully reflect realized reproductive investment, nor any associated, overall energetic strain.

We contend—irrespective of the future development of the zooplankton (cod larval prey) community in the Irish/Celtic Seas-English Channel Complex (Pitois & Fox, 2006)—that the projected increase in T in this area exceeding T_{up} (RCP4.5, 2006–2070) will seriously disturb

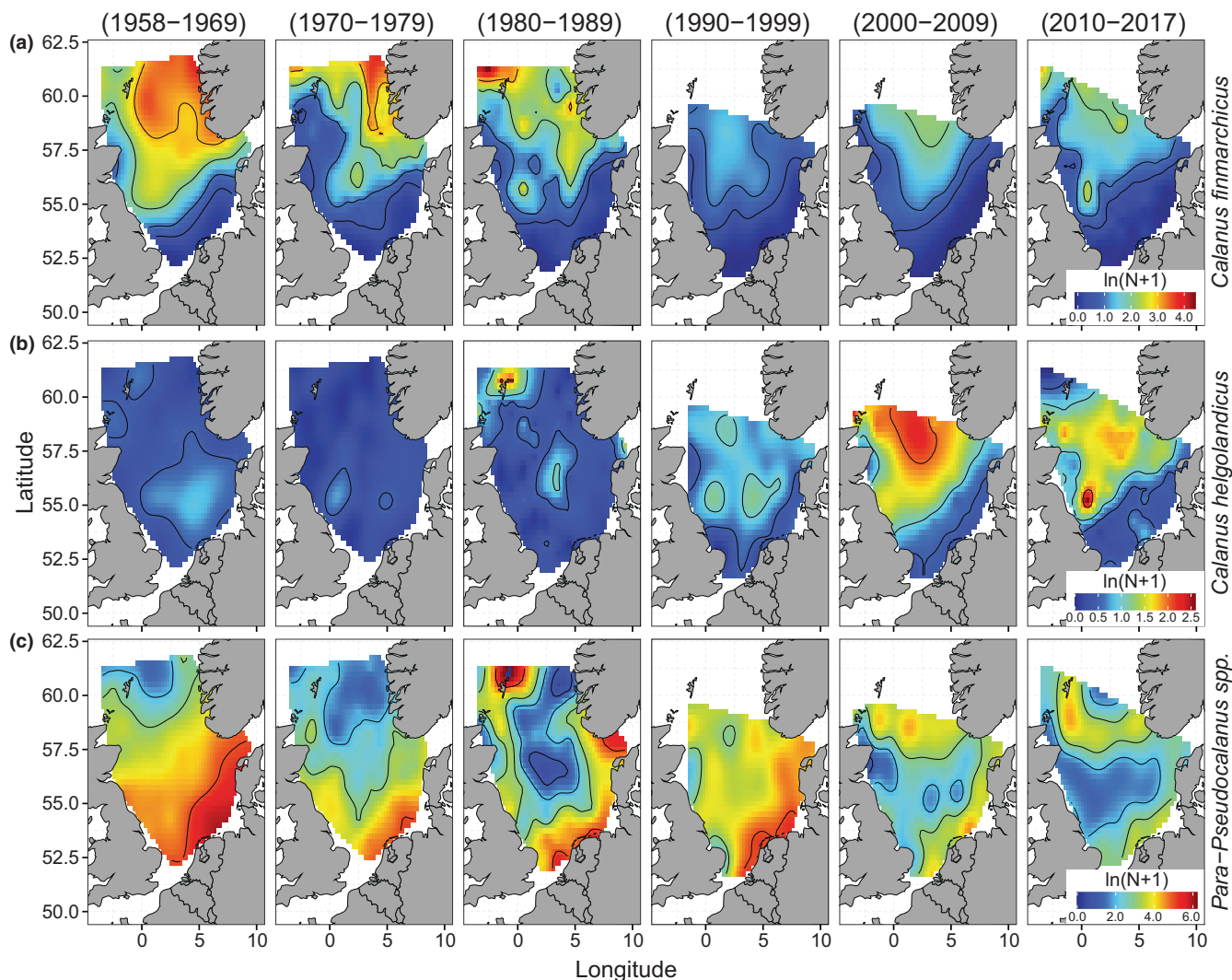## *Calanus finmarchicus*, *C. helgolandicus* and *Para-Pseudocalanus spp.* decadal distribution

FIGURE 9 Mean decadal distribution of *Calanus finmarchicus*, *C. helgolandicus* and *Para-Pseudocalanus* spp. abundance between April and August in the North Sea (1958–2017). Contour lines show the various isolines. All these ln-transformed data were extracted from the CPR data base.

local cod egg release. However, any healthy cod eggs advected into these waters might possibly survive at even higher *T* (Geffen et al., 2006). It seems reasonable to believe that the documented T_{up} is imprinted in the genes of *G. morhua* (Righton et al., 2010). Furthermore, this knife-edge threshold at 9.6 (±0.25)°C—supported by the study of van der Meeren and Ivannikov (2006) at the group level—tells that any coarsely rounding off to the nearest integer will only vaguely define future locations of suitable spawning grounds, despite that bottom temperature clines might be reasonably sharp, as documented at or near the present southern spawning grounds. Our findings in these respects are considered novel, moving beyond descriptive narratives or physiological extrapolations to real mechanistic observations at the individual level followed by climate projections to address the ultimate consequences for local spawning grounds.

In the relatively cooler North Sea, the present 19-year extension of the earlier investigation by Beaugrand et al. (2003) on North Sea

cod *SSB_yp3* (spawning stock biomass forward lagged by 3 years) vs. *C. finmarchicus* abundance illuminated the existence of a real link (r^2 = .43) in predator–prey dynamics. Despite this, for *C. finmarchicus*, brief and thereby unaccounted pulsed advection from the deep Norwegian Sea to the North Sea shelf might be an issue to study further (Heath et al., 1999; Sundby, 2000). Events of high fishing mortality—explored via complementary *Recruitment_yp1* (recruitment at year +1) analyses—did not jeopardize this finding, though the dominant problem with discards and overfishing persists, as further south in the study region (www.ices.dk). The combination of subarea-specific CPR and IBTS datasets (NW = Northwestern, S = Southern, VPa = Viking4a) evidenced local differences in copepod abundance and in *SSB_yp3_NW*, *SSB_yp3_S* and *SSB_yp3_VPa*, as well as in *Recruitment_yp1_NW*, *Recruitment_yp1_S* and *Recruitment_yp1_VPa*, with the S subarea doing poorly in recent times. However, *C. helgolandicus* is on the rise but this trend is, as illustrated, unfavourable

FIGURE 10 The long-term relationships (1960–2017) between *Calanus finmarchicus* abundance and spawning stock biomass (*SSB*) of cod in the North Sea. (a) Observed trends, where the dotted line shows the last study year (1998) by Beaugrand et al. (2003); and (b) the corresponding linear relationship (mean ± 95% confidence interval). *C. finmarchicus* abundance refers to April–August, extracted from the CPR data base. *SSB* is 3-year lagged. Regression line: $Y = 50.4 + 82.56 \times X$.
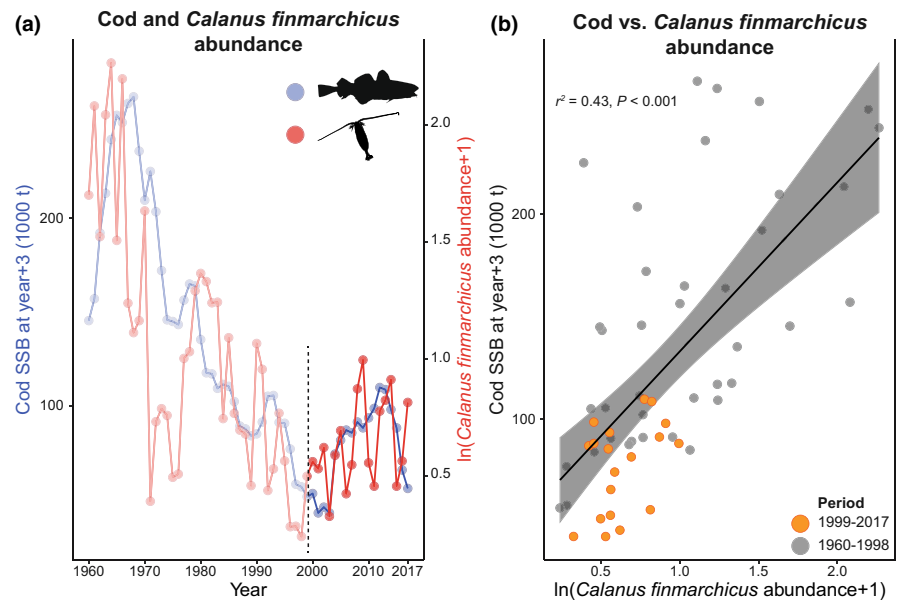
for cod productivity (Beaugrand et al., 2003; Sundby, 2000); *C. helgolandicus* generally peaks in abundance past the cod larval feeding season (Beaugrand & Ibanez, 2004; Bonnet et al., 2005). Another relevant point in this connection is also that the long-term average abundance of *C. helgolandicus* is, as demonstrated, about one order of magnitude lower than for *C. finmarchicus*. This part of our fine-resolved analysis (1978–2017) supplements a previous investigation limited to the southern (and central) North Sea (1974–2011) (Nicolas et al., 2014). Although the NW and VPa subareas give a more positive outlook in terms of copepod abundance, it is worth recognizing that generally little of the deviance (< ≈15%) is explained when split by subarea; the whole-ocean analysis generally showed significantly better explanatory power. As an example, in terms of *Recruitment_yp1_S* versus. copepod abundance, the current rank—in a declining order—goes from *C. finmarchicus* (positive influence) via *Para-Pseudocalanus* spp. (positive influence) to *C. helgolandicus* (negative influence), whereas Nicolas et al. (2014) showed an inverse pattern from *C. helgolandicus* via *Para-Pseudocalanus* to *C. finmarchicus*. Also, although *Para-Pseudocalanus* spp. appeared in our tests to be statistically uninfluenced by North Sea *SST*, these small copepods are evidently displaced northwards in this ocean basin, as seen for *C. finmarchicus* (Beaugrand et al., 2002; Sundby, 2000). Hence, we realized that the existence of pronounced collinearity between *T* and copepod category abundance generally hindered any true statistical insight in their individual role as predictors. Furthermore, at least the poor relationship between *Recruitment_yp1_V4a* and copepod categories may be due to a portion of cod recruits being in the adjacent Skagerrak (Wright et al., 2018). Nonetheless, the North Sea cod in the S subarea are certainly more at risk under on-going climate change than in the NW and V4a subareas but there are contributory factors to this scenario, such as locally altered fishing pressure (Engelhard et al., 2014). However, no direct evidence exists for related changes in adult migrations as such (Neat et al., 2014). The IBTS was launched a few years after the Gadoid Outburst in the cold 1960–1970s and the concurrent event of a historic peak in *C.*

finmarchicus abundance (Cushing, 1984). Thus, the relative role of the S subarea was probably even more prominent pre-IBTS when these warm water masses cooled due to natural long-term climate oscillations (Gullestad et al., 2020). So, altogether, our work highlights the high importance of long time series, documenting, as a clear example, that not only *SSB_yp3* but also *C. finmarchicus* abundance in the North Sea are today in a dire state; all recent 19 data points fell near the origin. However, more worrying is the reduced recruitment of North Sea cod since the late 1990s, although seeing indications of a weak improvement in *SSB* just now (ICES, 2022). In any case, infrequent incidences of highly successful recruitment play a paramount role for any subsequent rebuilding of stock size (Hutchings, 2000).

In the relatively cold Barents Sea, we addressed cod displacement distance (D_D) and speed (U_D)—a clearly understudied topic of special relevance today—as neither Barents Sea cod spawning temperature nor distribution of *C. finmarchicus* have yet changed substantially (Gullestad et al., 2020; Sandø et al., 2020; Sundby, 2000). This research action was inspired by previous analyses on coastal landing data indicating that the geographical distance between cod spawning grounds displaced southwards in a cold period and northwards in a warm period may sum up to a distance of 500 km (Langangen et al., 2019; Sundby & Nakken, 2008). We found that the variation in the centre of gravity (*CoG*) in the Barents Sea related to ice extent (Ingvaldsen & Gjøsæter, 2013; IPCC, 2021). Also, the switch in latitudinal position of large and small cod between summer and winter is explained by the fact that large cod migrate out of the Barents Sea in late winter to spawn on the coast (Sundby & Nakken, 2008). This said, the environmental temperature, represented by *Kola T* was an inadequate reflection of ambient *T*. So, mechanistically speaking, the indirect effect of ocean warming on D_D and U_D was not only totally dominating but also functioned as a cascading effect, seen by a reduced ice extent, an enlarged suitable feeding area (*SFA*), a larger total stock biomass (*TSB*) and then a pronounced increase in both D_D and U_D. However, in line with the general concept of lower
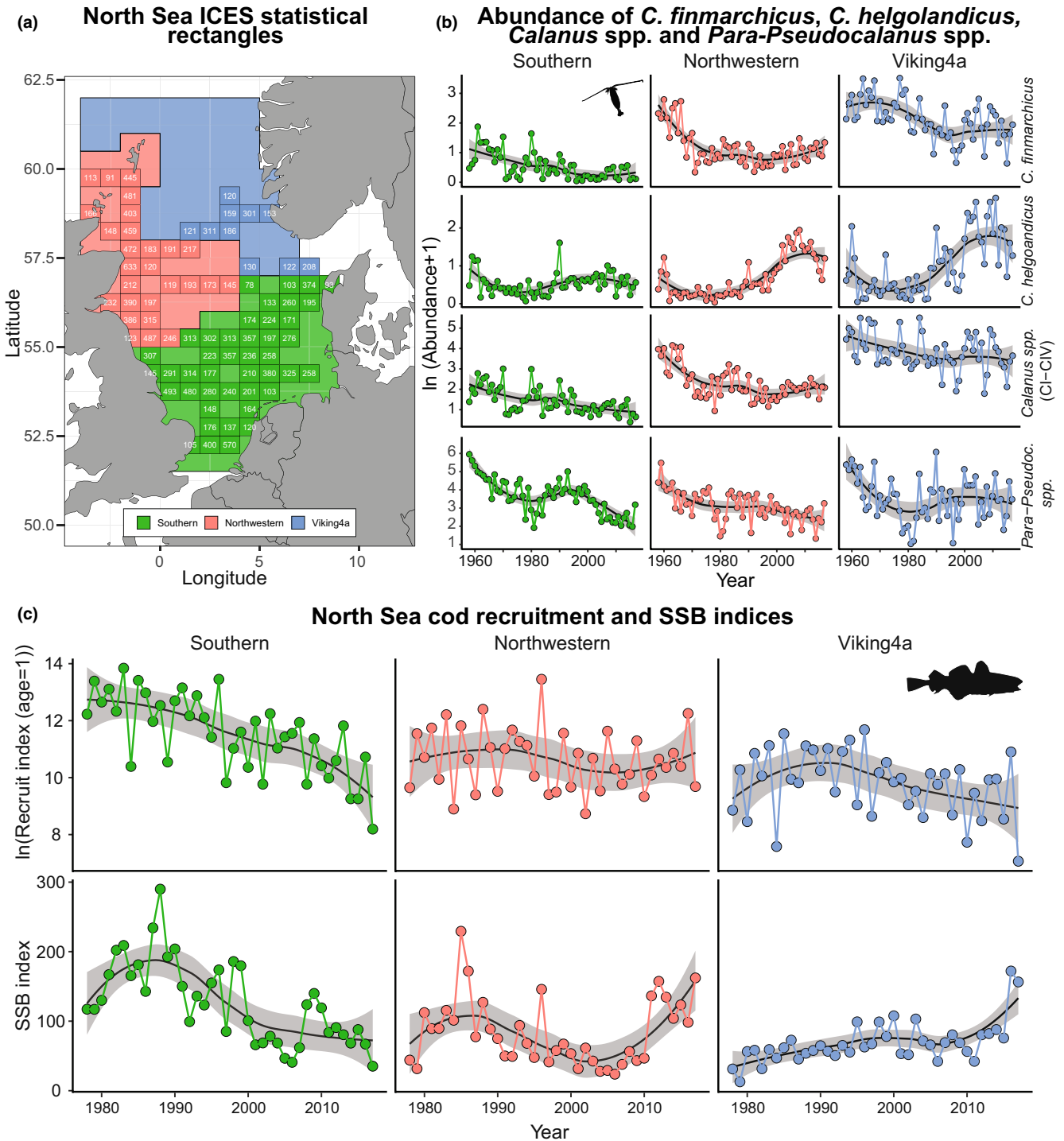
KJESBU ET AL.

FIGURE 11 Subarea-resolved time series on *Calanus finmarchicus*, *C. helgolandicus*, *C.* spp. (CI-CIV) and *Para-Pseudocalanus* spp. abundances (1958–2017) and the corresponding information on North Sea cod recruitment and spawning stock biomass (*SSB*) (1978–2017). (a) North Sea ICES statistical rectangles with grid cells, grouped into the southern, northwestern and Viking 4a subareas; (b) trends in abundance (mean ± SE) of the four copepod categories; and (c) recruitment-at-age-1-year and SSB indices for North Sea cod. Only CPR data (April–August) regularly sampled within ICES grid cells were considered. For North Sea cod, the data originate from the IBTS.

migration costs per unit body mass when body size increases (Jansen et al., 2021; Nøttestad et al., 1999; Schmidt-Nielsen, 1983), a statistically significant relationship between either D_D or U_D and *TSB* only applied for large cod. Because of this major contribution of *TSB* to D_D and U_D, an increase in *TSB* from, for instance, 1.5–4.5 million t, will

increase D_D and U_D by a factor of 1.64 and 1.72, respectively. These accelerated migration costs (Jørgensen & Fiksen, 2006; Nøttestad et al., 1999) might negatively affect reproductive investment, such as fecundity (dos Santos Schmidt et al., 2017; McBride et al., 2015). This consideration also relates to that spawning migratory cod do
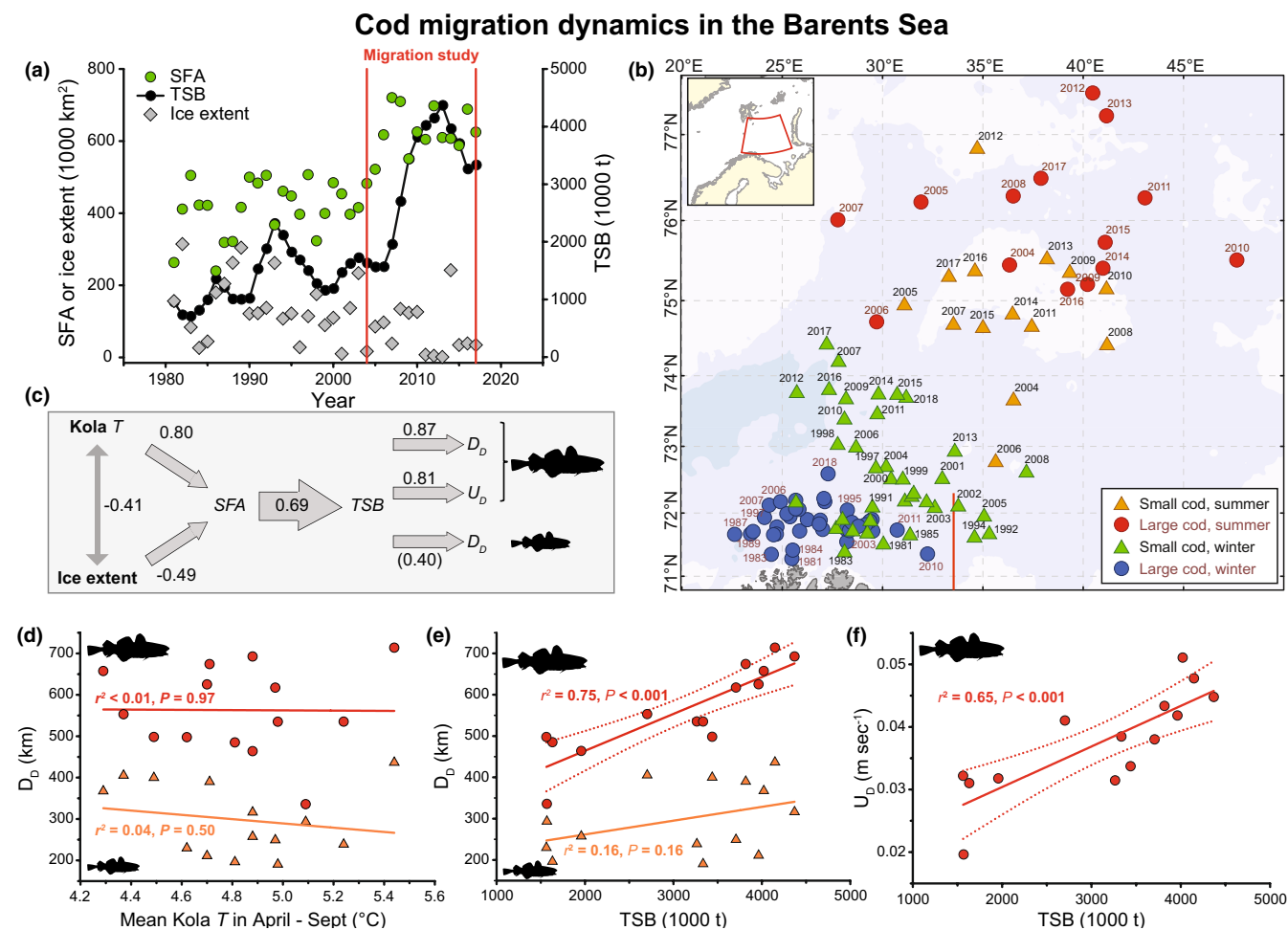
Cod migration dynamics in the Barents Sea

FIGURE 12 Seasonal migration dynamics of Barents Sea cod. (a) Consulted environmental drivers in the migration study (2004–2017/2018), in addition to Kola transect temperature (*Kola T*) (Figure 1b). The plotted time series for *SFA* (suitable feeding area), *TSB* (total stock biomass) and ice extent were for illustrative purposes extended back to 1981; (b) annual changes in the centre of gravity of Barents Sea cod during winter and summer by total length (*TL*) category. Line: Kola transect. The insert shows the surveyed area, in wintertime depending on ice extension (Ingvaldsen & Gjøsæter, 2013). Bathymetry, white: 0–200; grey: 200–400; blue: 400–600 m; (c) correlation coefficient flowchart between drivers and displacement length (D_D) and speed (U_D) for small ($30 \leq TL \leq 59$ cm) and large cod ($70 \leq TL \leq 99$ cm). *Kola T* is given as the mean value in April to September. Parenthesis: An insignificant relationship; (d) and (e) D_D regressed on *Kola T* and *TSB* for small and large Barents Sea cod, respectively. Upper regression line in (e): $Y = 286 + 0.089 \times X$; and (f) U_D regressed on *TSB* for large cod. Regression line: $Y = 1.74 \cdot 10^{-2} + 6.48 \cdot 10^{-6} \times X$.

not feed to any significant extent (Kjesbu et al., 1991). Another factor to consider is that the proximate player in question is *TSB*, a density-dependent factor, which is intimately linked to the adopted stock management regime, on top of the warmer climate (Kjesbu et al., 2014). Conversely, examples of extremely long Barents Sea cod migration southwards in historic cold periods (Sundby & Nakken, 2008) may well relate to other causal mechanisms, such as better recruitment in relatively warmer waters (Ellertsen et al., 1989; Planque & Frédou, 1999) translating to a gradual strengthening of the southernmost spawning grounds along the Norwegian coast (Sundby & Nakken, 2008). Nevertheless, the location of the ice edge and thereby of the polar-front-associated Barents Sea capelin (*Mallotus villosus*, Osmeridae) (Ingvaldsen & Gjøsæter, 2013)—a key cod food item (Kjesbu et al., 2014)—is certainly an issue (Kjesbu et al., 2022). All aspects considered, this high-latitude example illustrates that any further increased migration distance and speed to

coastal spawning grounds may turn energetically supercritical under the current extreme northward displacement of feeding areas.

5 | CONCLUSION

Our research has shown that understanding and predicting (or projecting) population (stock) persistence under anthropogenic climate change should be based on revealing the key, local regulatory mechanisms. This viewpoint is further underlined in this article by concentrating on the life-history trait-based 'weak link' (critical sensitivity attribute)—using Atlantic cod as a template species—within each of the three Northeast Atlantic regions (50–80° N) currently addressed. Such an approach might, however, be criticized in cases where a series of sensitivity attributes in combination turn critical rather than each singularly, a common argument in climate
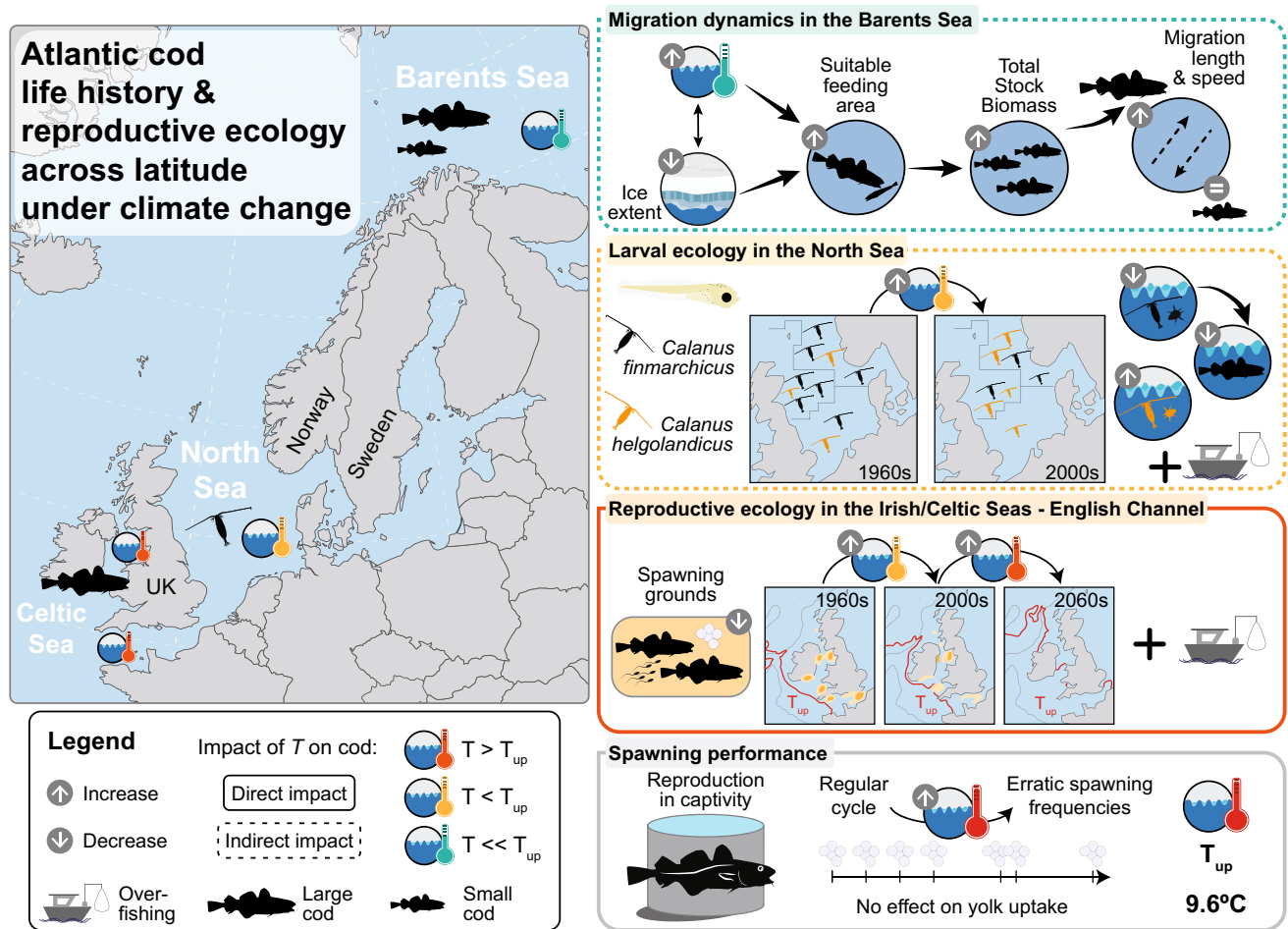
FIGURE 13 Overview of study region including ocean basins, the four research topics addressed, and the main findings in this investigation on life-history and reproductive challenges encountered by Northeast Atlantic cod stocks under on-going climate change.

impact assessments using expert scorings. Thus, our endeavour should be considered as an alternative, where the strength lies in thorough, quantitative investigations of key traits and their drivers resulting in findings of clear importance for future cod stock productivity (Figure 13). These novel results were made possible by running dedicated experiments, consulting extensive data bases and accessing and building upon a wealth of knowledge gathered by generations of researchers within different branches of marine science.

AUTHOR CONTRIBUTIONS

O.S.K. and S.S. involved in conceptualization; A.B.S. and M.S.M. provided the climate models; D.G.J. and E.S. provided the CPR data; P.J.W. and E.S. provided the IBTS data; M.A., E.S., A.B.S., O.S.K. and K.B. involved in visualization; O.S.K., A.T. and C.T.M. did the experiments; O.S.K., A.B.S. and K.B. provided the CTD and CoG data; G.H., F.B.V., G.O., B.J.M.A., M.F. and J.E.S. involved in supervision; G.H., F.B.V. and O.S.K. acquired the funding; O.S.K. and S.S wrote the original draft; O.S.K., M.A., S.S., A.B.S., E.S., P.J.W., C.T.M., F.B.V. and G.H reviewed and edited the manuscript.

DATA AVAILABILITY STATEMENT

All data—including any links to external databases—are accessible in the online Supporting Information file.

ORCID

Olav Sigurd Kjesbu https://orcid.org/0000-0002-8651-6838
Maud Alix https://orcid.org/0000-0002-2365-9188
Anne Britt Sandø https://orcid.org/0000-0002-2373-2808
Bridie J. M. Allan https://orcid.org/0000-0002-5991-9711
Svein Sundby https://orcid.org/0000-0002-0815-9740

REFERENCES

Alix, M., Kjesbu, O. S., & Anderson, K. C. (2020). From gametogenesis to spawning: How climate-driven warming affects teleost reproductive biology. *Journal of Fish Biology, 97*, 607–632. https://doi.org/10.1111/jfb.14439

Barneche, D. R., Robertson, D. R., White, C. R., & Marshall, D. J. (2018). Fish reproductive-energy output increases disproportionately with body size. *Science, 360*(6389), 642–644. https://doi.org/10.1126/science.aao6868

Beaugrand, G., Brander, K. M., Lindley, J. A., Souissi, S., & Reid, P. C. (2003). Plankton effect on cod recruitment in the North Sea. *Nature, 426*(6967), 661–664. https://doi.org/10.1038/nature02164

Beaugrand, G., & Ibanez, F. (2004). Monitoring marine plankton ecosystems. II: Long-term changes in North Sea calanoid copepods in relation to hydro-climatic variability. *Marine Ecology Progress Series, 284*, 35–47. https://doi.org/10.3354/meps284035

Beaugrand, G., Reid, P. C., Ibanez, F., Lindley, J. A., & Edwards, M. (2002). Reorganization of North Atlantic marine copepod biodiversity and climate. *Science, 296*(5573), 1692–1694. https://doi.org/10.1126/science.1071329

Bentsen, M., Bethke, I., Debernard, J. B., Iversen, T., Kirkevåg, A., Seland, Ø., Drange, H., Roelandt, C., Seierstad, I. A., Hoose, C., & Kristjánsson, J. E. (2013). The Norwegian earth system model, NorESM1-M–part 1: Description and basic evaluation of the physical climate. *Geoscientific Model Development, 6*, 687–720. https://doi.org/10.5194/gmd-6-687-2013

Boitsov, V. D., Karsakov, A. L., & Trofimov, A. G. (2012). Atlantic water temperature and climate in the Barents Sea, 2000-2009. *ICES Journal of Marine Science, 69*, 833–840. https://doi.org/10.1093/icesjms/fss075

Bonnet, D., Richardson, A., Harris, R., Hirst, A., Beaugrand, G., Edwards, M., Ceballos, S., Diekman, R., Lopez-Urrutia, A., Valdes, L., Carlotti, F., Molinero, J. C., Weikert, H., Greve, W., Lucic, D., Albaina, A., Yahia, N. D., Umani, S. F., Miranda, A., ... de Puelles, M. L. F. (2005). An overview of *Calanus helgolandicus* ecology in European waters. *Progress in Oceanography, 65*, 1–53. https://doi.org/10.1016/j.pocean.2005.02.002

Brander, K. (2005). Spawning and life history information for North Atlantic cod stocks. *ICES Cooperative Research Report* No. 274. 152pp. https://www.ices.dk/sites/pub/Publication%20Reports/Cooperative%20Research%20Report%20(CRR)/CRR274.pdf

Brander, K. (2019). Cod and climate change. In G. A. Rose (Eds.), *Atlantic cod: A bio-ecology* (pp. 337–384). Wiley Blackwell.

Brawn, V. M. (1962). Reproductive behaviour of the cod (*Gadus callarias* L.). *Behaviour, 18*, 177–198.

Carton, J. A., & Giese, B. S. (2008). A reanalysis of ocean climate using simple ocean data assimilation (SODA). *Monthly Weather Review, 136*, 2999–3017. https://doi.org/10.1175/2007mwr1978.1

Chambers, R. C., & Leggett, W. C. (1996). Maternal influences on variation in egg sizes in temperate marine fishes. *American Zoologist, 36*, 180–196. https://doi.org/10.1093/icb/36.2.180

Charitonidou, K., Kjesbu, O. S., Nunes, C., Angelico, M. M., Dominguez-Petit, R., Garabana, D., & Ganias, K. (2022). Linking the dynamic organization of the ovary with spawning dynamics in pelagic fishes. *Marine Biology, 169*(4), Article 47. https://doi.org/10.1007/s00227-022-04032-z

Cushing, D. H. (1984). The gadoid outburst in the North Sea. *ICES Journal of Marine Science, 41*, 159–166. https://doi.org/10.1093/icesjms/41.2.159

Dahlke, F. T., Wohlrab, S., Butzin, M., & Pörtner, H. O. (2020). Thermal bottlenecks in the life cycle define climate vulnerability of fish. *Science, 369*(6499), 65–70. https://doi.org/10.1126/science.aaz3658

Davie, A., Porter, M. J. R., Bromage, N. R., & Migaud, H. (2007). The role of seasonally altering photoperiod in regulating physiology in Atlantic cod (*Gadus morhua*). Part I. sexual maturation. *Canadian Journal of Fisheries and Aquatic Sciences, 64*(1), 84–97. https://doi.org/10.1139/f06-169

dos Santos Schmidt, T. C., Slotte, A., Kennedy, J., Sundby, S., Johannessen, A., Óskarsson, G. J., Kurita, Y., Stenseth, N. C., & Kjesbu, O. S. (2017). Oogenesis and reproductive investment of Atlantic herring are functions of not only present but long-ago environmental influences as well. *Proceedings of the National Academy of Sciences of the United States of America, 114*, 2634–2639. https://doi.org/10.1073/pnas.1700349114

Drinkwater, K. F. (2005). The response of Atlantic cod (*Gadus morhua*) to future climate change. *ICES Journal of Marine Science, 62*, 1327–1337. https://doi.org/10.1016/j.icejms.2005.05.015

Ellertsen, B., Fossum, P., Solemdal, P., & Sundby, S. (1989). Relation between temperature and survival of eggs and first-feeding larvae of Northeast Arctic cod (*Gadus morhua* L.). *Rapportes et Procès-Verbaux Réunions du Conseil International pour l' Exploration de la Mer, 191*, 209–219.

Engelhard, G. H., Righton, D. A., & Pinnegar, J. K. (2014). Climate change and fishing: A century of shifting distribution in North Sea cod. *Global Change Biology, 20*, 2473–2483. https://doi.org/10.1111/gcb.12513

Free, C. M., Thorson, J. T., Pinsky, M. L., Oken, K. L., Wiedenmann, J., & Jensen, O. P. (2019). Impacts of historical warming on marine fisheries production. *Science, 363*(6430), 979–983. https://doi.org/10.1126/science.aau1758

Geffen, A. J., Fox, C. J., & Nash, R. D. M. (2006). Temperature-dependent development rates of cod *Gadus morhua* eggs. *Journal of Fish Biology, 69*, 1060–1080.

Gerritsen, H. (2018). *mapplots: Data Visualisation on Maps*. R package version 1.5.1 https://CRAN.R-project.org/package=mapplots

Godø, O. R., & Michalsen, K. (2000). Migratory behaviour of north-East Arctic cod, studied by use of data storage tags. *Fisheries Research, 48*, 127–140. https://doi.org/10.1016/S0165-7836(00)00177-6

Gullestad, P., Sundby, S., & Kjesbu, O. S. (2020). Management of transboundary and straddling fish stocks in the Northeast Atlantic in view of climate-induced shifts in spatial distribution. *Fish and Fisheries, 21*, 1008–1026. https://doi.org/10.1111/faf.12485

Hansen, Ø. J., Puvanendran, V., & Bangera, R. (2016). Broodstock diet with water and astaxanthin improve condition and egg output of brood fish and larval survival in Atlantic cod, *Gadus morhua* L. *Aquaculture Research, 47*, 819–829. https://doi.org/10.1111/are.12540

Hare, J. A., Morrison, W. E., Nelson, M. W., Stachura, M. M., Teeters, E. J., Griffis, R. B., Alexander, M. A., Scott, J. D., Alade, L., Bell, R. J., Chute, A. S., Curti, K. L., Curtis, T. H., Kircheis, D., Kocik, J. F., Lucey, S. M., McCandless, C. T., Milke, L. M., Richardson, D. E., ... Griswold, C. A. (2016). A vulnerability assessment of fish and invertebrates to climate change on the northeast US continental shelf. *PLoS One, 11*(2), e0146756. https://doi.org/10.1371/journal.pone.0146756

Heath, M. R., Backhaus, J. O., Richardson, K., McKenzie, E., Slagstad, D., Beare, D., Dunn, J., Fraser, J. G., Gallego, A., & Hainbucher, D. (1999). Climate fluctuations and the spring invasion of the North Sea by *Calanus finmarchicus*. *Fisheries Oceanography, 8*, 163–176.

Hiemstra, P. H., Pebesma, E. J., Twenhöfel, C. J., & Heuvelink, G. B. (2009). Real-time automatic interpolation of ambient gamma dose rates from the Dutch radioactivity monitoring network. *Computers*

& *Geosciences*, *35*, 1711–1721. https://doi.org/10.1016/j.cageo.2008.10.011

Holmes, S. J., Millar, C. P., Fryer, R. J., & Wright, P. J. (2014). Gadoid dynamics: Differing perceptions when contrasting stock vs. population trends and its implications to management. *ICES Journal of Marine Science*, *71*, 1433–1442. https://doi.org/10.1093/icesjms/fsu075

Huang, B., Thorne, P. W., Banzon, V. F., Boyer, T., Chepurin, G., Lawrimore, J. H., Menne, M. J., Smith, T. M., Vose, R. S., & Zhang, H.-M. (2017). NOAA extended Reconstructed Sea surface temperature (ERSST), Version 5 [Subset: 1958-2020]. *NOAA National Centers for Environmental Information*. https://doi.org/10.7289/V5T72FNM. [Accessed date : 18 August 2021]

Hutchings, J. A. (2000). Collapse and recovery of marine fishes. *Nature*, *406*(6798), 882–885. https://doi.org/10.1038/35022565

ICES. (2015). *Report of the Benchmark Workshop on North Sea Stocks (WKNSEA), 2–6 February 2015, Copenhagen, Denmark ICES CM 2015/ACOM:32*. https://archimer.ifremer.fr/doc/00586/69828/67724.pdf

ICES. (2017). *Advice on fishing opportunities, catch, and effort Greater North Sea Ecoregion*. Cod (*Gadus morhua*) in Subarea 4, Division 7.d, and Subdivision 20 (North Sea, eastern English Channel, Skagerrak) [ICES Advice: Recurrent advice]. https://doi.org/10.17895/ices.pub.3526

ICES. (2020). Arctic fisheries working group (AFWG). *ICES Scientific Reports*, *2*(52), 577. https://doi.org/10.17895/ices.pub.6092

ICES. (2022). *Advice on fishing opportunities, catch, and effort Greater North Sea Ecoregion. Cod (Gadus morhua) in Subarea 4, Division 7.d, and Subdivision 20 (North Sea, eastern English Channel, Skagerrak) [ICES Advice: Recurrent advice]*. https://doi.org/10.17895/ices.advice.19447880

Ingvaldsen, R. B., & Gjøsæter, H. (2013). Responses in spatial distribution of Barents Sea capelin to changes in stock size, ocean temperature and ice cover. *Marine Biology Research*, *9*, 867–877. https://doi.org/10.1080/17451000.2013.775450

Inpixon. (2022). https://systatsoftware.com/

IPCC. (2021). Summary for policymakers. In V. Masson-Delmotte, P. Zhai, A. Pirani, S. L. Connors, C. Péan, S. Berger, N. Caud, Y. Chen, L. Goldfarb, M. I. Gomis, M. Huang, K. Leitzell, E. Lonnoy, J. B. R. Matthews, T. K. Maycock, T. Waterfield, O. Yelekçi, R. Yu, & B. Zhou (Eds.), *Climate change 2021: The physical science basis. Contribution of working group I to the sixth assessment report of the intergovernmental panel on climate change* (pp. 3–32). Cambridge University Press. https://doi.org/10.1017/9781009157896.001

Jakobsen, T., Korsbrekke, K., Mehl, S., & Nakken, O. (1997). *Norwegian combined acoustic and bottom trawl surveys for demersal fish in the Barents Sea during winter. ICES CM 1997/Y:17*. https://www.ices.dk/sites/pub/CM%20Doccuments/1997/Y/1997_Y17.pdf

Jakobsson, J., Astthorsson, O. S., Beverton, R. J. H., Bjørnsson, B., Daan, N., Frank, K. T., Meincke, J., Rothschild, B., Sundby, S., & Tilseth, S. (Eds.) (1994). *Cod and climate change. Proceedings of a symposium held in Reykjavík, 23–27 august 1993* (Vol. *198*, pp.698). ICES Marine Science Symposia.

Jansen, T., Slotte, A., Schmidt, T. C. D., Sparrevohn, C. R., Jacobsen, J. A., & Kjesbu, O. S. (2021). Bioenergetics of egg production in Northeast Atlantic mackerel changes the perception of fecundity type and annual trends in spawning stock biomass. *Progress in Oceanography*, *198*, 102658. https://doi.org/10.1016/j.pocean.2021.102658

Jørgensen, C., & Fiksen, Ø. (2006). State-dependent energy allocation in cod (*Gadus morhua*). *Canadian Journal of Fisheries and Aquatic Sciences*, *63*, 186–199. https://doi.org/10.1139/f05-209

Jutfelt, F., Norin, T., Ern, R., Overgaard, J., Wang, T., McKenzie, D. J., Lefevre, S., Nilsson, G. E., Metcalfe, N. B., Hickey, A. J. R., Brijs, J., Speers-Roesch, B., Roche, D. G., Gamperl, A. K., Raby, G. D., Morgan, R., Esbaugh, A. J., Gräns, A., Axelsson, M., ... Clark, T. D. (2018). Oxygen- and capacity-limited thermal tolerance: Blurring

ecology and physiology. *Journal of Experimental Biology*, *221*(1), jeb169615. https://doi.org/10.1242/jeb.169615

Kassambara, A. (2020). Ggpubr: 'ggplot2' based publication ready plots. R package version 0.4.0. https://CRAN.R-project.org/package=ggpubr

Kjesbu, O. S. (1989). The spawning activity of cod, *Gadus morhua* L. *Journal of Fish Biology*, *34*, 195–206. https://doi.org/10.1111/j.1095-8649.1989.tb03302.x

Kjesbu, O. S., Bogstad, B., Devine, J. A., Gjøsæter, H., Howell, D., Ingvaldsen, R. B., Nash, R. D. M., & Skjæraasen, J. E. (2014). Synergies between climate and management for Atlantic cod fisheries at high latitudes. *Proceedings of the National Academy of Sciences of the United States of America*, *111*, 3478–3483. https://doi.org/10.1073/pnas.1316342111

Kjesbu, O. S., Klungsøyr, J., Kryvi, H., Witthames, P. R., & Greer Walker, M. (1991). Fecundity, atresia, and egg size of captive Atlantic cod (*Gadus morhua*) in relation to proximate body composition. *Canadian Journal of Fisheries and Aquatic Sciences*, *48*, 2333–2343. https://doi.org/10.1139/f91-274

Kjesbu, O. S., Kryvi, H., & Norberg, B. (1996). Oocyte size and structure in relation to blood plasma steroid hormones in individually monitored, spawning Atlantic cod. *Journal of Fish Biology*, *49*, 1197–1215. https://doi.org/10.1111/j.1095-8649.1996.tb01789.x

Kjesbu, O. S., Righton, D., Krüger-Johnsen, M., Thorsen, A., Michalsen, K., Fonn, M., & Witthames, P. R. (2010). Thermal dynamics of ovarian maturation in Atlantic cod (*Gadus morhua*). *Canadian Journal of Fisheries and Aquatic Sciences*, *67*(4), 605–625. https://doi.org/10.1139/f10-011

Kjesbu, O. S., Solemdal, P., Bratland, P., & Fonn, M. (1996). Variation in annual egg production in individual captive Atlantic cod (*Gadus morhua*). *Canadian Journal of Fisheries and Aquatic Sciences*, *53*(3), 610–620. https://doi.org/10.1139/cjfas-53-3-610

Kjesbu, O. S., Sundby, S., Sandø, A. B., Alix, M., Hjøllo, S. S., Tiedemann, M., Skern-Mauritzen, M., Junge, C., Fossheim, M., Broms, C. T., Søvik, G., Zimmermann, F., Nedreaas, K., Eriksen, E., Höffle, H., Hjelset, A. M., Kvamme, C., Reecht, Y., Knutsen, H., ... Huse, G. (2022). Highly mixed impacts of near-future climate change on stock productivity proxies in the north East Atlantic. *Fish and Fisheries*, *23*, 601–615. https://doi.org/10.1111/faf.12635

Kjesbu, O. S., Witthames, P. R., Solemdal, P., & Walker, M. G. (1998). Temporal variations in the fecundity of Arcto-Norwegian cod (*Gadus morhua*) in response to natural changes in food and temperature. *Journal of Sea Research*, *40*, 303–321. https://doi.org/10.1016/s1385-1101(98)00029-x

Kurlansky, M. (2011). *Cod: A biography of the fish that changed the world*. Walker and Company.

Langangen, Ø., Farber, L., Stige, L. C., Diekert, F. K., Barth, J. M. I., Matschiner, M., Berg, P. R., Star, B., Stenseth, N. C., Jentoft, S., & Durant, J. M. (2019). Ticket to spawn: Combining economic and genetic data to evaluate the effect of climate and demographic structure on spawning distribution in Atlantic cod. *Global Change Biology*, *25*, 134–143. https://doi.org/10.1111/gcb.14474

Large, W. G., & Yeager, S. G. (2009). The global climatology of an interannually varying air-sea flux data set. *Climate Dynamics*, *33*, 341–364. https://doi.org/10.1007/s00382-008-0441-3

Levesque, D. L., & Marshall, K. E. (2021). Do endotherms have thermal performance curves? *Journal of Experimental Biology*, *224*(3), jeb141309. https://doi.org/10.1242/jeb.141309

Little, A. G., Loughland, I., & Seebacher, F. (2021). What do warming waters mean for fish physiology and fisheries? *Journal of Fish Biology*, *98*, 1493. https://doi.org/10.1111/jfb.14803

Marshall, C. T., Needle, C. L., Thorsen, A., Kjesbu, O. S., & Yaragina, N. A. (2006). Systematic bias in estimates of reproductive potential of an Atlantic cod (*Gadus morhua*) stock: Implications for stock-recruit theory and management. *Canadian Journal of Fisheries and Aquatic Sciences*, *63*, 980–994. https://doi.org/10.1139/f05-270

Marteinsdottir, G., & Rose, G. A. (2019). Atlantic cod: Origin and evolution. In G. A. Rose (Ed.), *Atlantic cod: A bio-ecology* (pp. 7–25). John Wiley & Sons Ltd.

Marteinsdottir, G., & Steinarsson, A. (1998). Maternal influence on the size and viability of Iceland cod *Gadus morhua* eggs and larvae. *Journal of Fish Biology, 52,* 1241–1258. https://doi.org/10.1006/jfbi.1998.0670

McBride, R. S., Somarakis, S., Fitzhugh, G. R., Albert, A., Yaragina, N. A., Wuenschel, M. J., Alonso-Fernandez, A., & Basilone, G. (2015). Energy acquisition and allocation to egg production in relation to fish reproductive strategies. *Fish and Fisheries, 16,* 23–57. https://doi.org/10.1111/faf.12043

Michalsen, K., Dalpadado, D., Eriksen, E., Gjøsæter, H., Ingvaldsen, R., Johannesen, E., Jørgensen, L., Knutsen, T., Prozorkevich, D., & Skern-Mauritzen, M. (2011). The joint Norwegian-Russian ecosystem survey: Overview and lessons learned. In T. Haug, A. Dolgov, K. Drevetnyak, I. Røttingen, K. Sunnanå, & O. Titov (Eds.), *Climate change and effects on the Barents Sea marine living resources. Proceedings of the 15th Russian-Norwegian symposium, Longyearbyen, Norway, 7–8 September 2011* (pp. 247–272). Institute of Marine Research.

Miranda, L. A., Chalde, T., Elisio, M., & Strüssmann, C. A. (2013). Effects of global warming on fish reproductive endocrine axis, with special emphasis in pejerrey *Odontesthes bonariensis. General and Comparative Endocrinology, 192,* 45–54. https://doi.org/10.1016/j.ygcen.2013.02.034

Morley, J. W., Selden, R. L., Latour, R. J., Frölicher, T. L., Seagraves, R. J., & Pinsky, M. L. (2018). Projecting shifts in thermal habitat for 686 species on the north American continental shelf. *PLoS One, 13*(5), e0196127. https://doi.org/10.1371/journal.pone.0196127

Nash, R. D. M., Pilling, G. M., Kell, L. T., Schön, P. J., & Kjesbu, O. S. (2010). Investment in maturity-at-age and -length in Northeast Atlantic cod stocks. *Fisheries Research, 104,* 89–99. https://doi.org/10.1016/j.fishres.2010.03.001

Neat, F. C., Bendall, V., Berx, B., Wright, P. J., Cuaig, M. O., Townhill, B., Schon, P. J., Lee, J., & Righton, D. (2014). Movement of Atlantic cod around the British Isles: Implications for finer scale stock management. *Journal of Applied Ecology, 51,* 1564–1574. https://doi.org/10.1111/1365-2664.12343

Nicolas, D., Rochette, S., Llope, M., & Licandro, P. (2014). Spatio-temporal variability of the North Sea cod recruitment in relation to temperature and zooplankton. *PLoS One, 9*(2), e88447. https://doi.org/10.1371/journal.pone.0088447

Nøttestad, L., Giske, J., Holst, J. C., & Huse, G. (1999). A length-based hypothesis for feeding migrations in pelagic fish. *Canadian Journal of Fisheries and Aquatic Sciences, 56,* 26–34. https://doi.org/10.1139/cjfas-56-S1-26

Ouellet, P., Lambert, Y., & Berube, I. (2001). Cod egg characteristics and viability in relation to low temperature and maternal nutritional condition. *ICES Journal of Marine Science, 58,* 672–686. https://doi.org/10.1006/jmsc.2001.1065

Payne, M. R., Kudahl, M., Engelhard, G. H., Peck, M. A., & Pinnegar, J. K. (2021). Climate risk to European fisheries and coastal communities. *Proceedings of the National Academy of Sciences, 118*(40), e2018086118. https://doi.org/10.1073/pnas.2018086118

Pershing, A. J., Alexander, M. A., Hernandez, C. M., Kerr, L. A., Le Bris, A., Mills, K. E., Nye, J. A., Record, N. R., Scannell, H. A., Scott, J. D., Sherwood, G. D., & Thomass, A. C. (2015). Slow adaptation in the face of rapid warming leads to collapse of the Gulf of Maine cod fishery. *Science, 350*(6262), 809–812. https://doi.org/10.1126/science.aac9819

Pitois, S. G., & Fox, C. J. (2006). Long-term changes in zooplankton biomass concentration and mean size over the northwest European shelf inferred from continuous plankton recorder data. *ICES Journal of Marine Science, 63,* 785–798. https://doi.org/10.1016/j.icesjms.2006.03.009

Plack, P. A., Pritchard, D. J., & Fraser, N. W. (1971). Egg proteins in cod serum. *The Biochemical Journal, 121,* 847–856.

Planque, B., & Frédou, T. (1999). Temperature and the recruitment of Atlantic cod (*Gadus morhua*). *Canadian Journal of Fisheries and Aquatic Sciences, 56,* 2069–2077. https://doi.org/10.1139/cjfas-56-11-2069

Poloczanska, E. S., Brown, C. J., Sydeman, W. J., Kiessling, W., Schoeman, D. S., Moore, P. J., Brander, K., Bruno, J. F., Buckley, L. B., Burrows, M. T., Duarte, C. M., Halpern, B. S., Holding, J., Kappel, C. V., O'Connor, M. I., Pandolfi, J. M., Parmesan, C., Schwing, F., Thompson, S. A., & Richardson, A. J. (2013). Global imprint of climate change on marine life. *Nature Climate Change, 3,* 919–925. https://doi.org/10.1038/nclimate1958

Pörtner, H. O., Bock, C., Knust, R., Lannig, G., Lucassen, M., Mark, F. C., & Sartoris, F. J. (2008). Cod and climate in a latitudinal cline: Physiological analyses of climate effects in marine fishes. *Climate Research, 37,* 253–270. https://doi.org/10.3354/cr00766

Pörtner, H. O., Bock, C., & Mark, F. C. (2017). Oxygen- and capacity-limited thermal tolerance: Bridging ecology and physiology. *Journal of Experimental Biology, 220,* 2685–2696. https://doi.org/10.1242/jeb.134585

Pörtner, H. O., & Farrell, A. P. (2008). Physiology and climate change. *Science, 322*(5902), 690–692. https://doi.org/10.1126/science.1163156

R Core Team. (2019). *R: A Language and Environment for Statistical Computing.* R foundation for statistical computing http://www.R-project.org/

Rayner, N. A., Brohan, P., Parker, D. E., Folland, C. K., Kennedy, J. J., Vanicek, M., Ansell, T. J., & Tett, S. F. B. (2006). Improved analyses of changes and uncertainties in sea surface temperature measured in situ since the mid-nineteenth century: The HadSST2 dataset. *Journal of Climate, 19,* 446–469. https://doi.org/10.1175/jcli3637.1

Richardson, A. J., Walne, A. W., John, A. W. G., Jonas, T. D., Lindley, J. A., Sims, D. W., Stevens, D., & Witt, M. (2006). Using continuous plankton recorder data. *Progress in Oceanography, 68,* 27–74. https://doi.org/10.1016/j.pocean.2005.09.011

Righton, D. A., Andersen, K. H., Neat, F., Thorsteinsson, V., Steingrund, P., Svedäng, H., Michalsen, K., Hinrichsen, H. H., Bendall, V., Neuenfeldt, S., Wright, P., Jonsson, P., Huse, G., van der Kooij, J., Mosegaard, H., Hüssy, K., & Metcalfe, J. (2010). Thermal niche of Atlantic cod *Gadus morhua*: Limits, tolerance and optima. *Marine Ecology Progress Series, 420,* 1–13. https://doi.org/10.3354/meps08889

Rollefsen, G. (1934). The cod otolith as a guide to race, sexual development and mortality. *Rapports et Procès-verbaux des Réunions du Conseil International pour l'Exploration de la Mer, 88*(2), 1–5.

Sandø, A. B., Johansen, G. O., Aglen, A., Stiansen, J. E., & Renner, A. H. H. (2020). Climate change and new potential spawning sites for Northeast Arctic cod. *Frontiers in Marine Science, 7,* 28. https://doi.org/10.3389/fmars.2020.00028

Sandø, A. B., Mousing, E. A., Budgell, W. P., Hjøllo, S. S., Skogen, M. D., & Ådlandsvik, B. (2021). Barents Sea plankton production and controlling factors in a fluctuating climate. *ICES Journal of Marine Science, 78,* 1999–2016. https://doi.org/10.1093/icesjms/fsab067

Schmidt-Nielsen, K. (1983). *Animal physiology: Adaptation and environment* (Third Edition ed.). Cambridge University Press.

Servili, A., Canario, A. V. M., Mouchel, O., & Munoz-Cueto, J. A. (2020). Climate change impacts on fish reproduction are mediated at multiple levels of the brain-pituitary-gonad axis. *General and Comparative Endocrinology, 291,* 113439. https://doi.org/10.1016/j.ygcen.2020.113439

Shchepetkin, A. F., & McWilliams, J. C. (2005). The regional oceanic modeling system (ROMS): A split-explicit, free-surface, topography-following-coordinate oceanic model. *Ocean Modelling, 9,* 347–404. https://doi.org/10.1016/j.ocemod.2004.08.002

Sokal, R. R., & Rohlf, F. J. (1981). Biometry. In *The principles and practice of statistics in biological research* (Second Edition ed.). W.H. Freeman and Company.

Sundby, S. (2000). Recruitment of Atlantic cod stocks in relation to temperature and advection of copepod populations. *Sarsia*, 85, 277–298. https://doi.org/10.1080/00364827.2000.10414580

Sundby, S., & Nakken, O. (2008). Spatial shifts in spawning habitats of Arcto-Norwegian cod related to multidecadal climate oscillations and climate change. *ICES Journal of Marine Science*, 65, 953–962. https://doi.org/10.1093/icesjms/fsn085

Thorsen, A., & Kjesbu, O. S. (2001). A rapid method for estimation of oocyte size and potential fecundity in Atlantic cod using a computer-aided particle analysis system. *Journal of Sea Research*, 46, 295–308. https://doi.org/10.1016/s1385-1101(01)00090-9

Thorsen, A., Kjesbu, O. S., Fyhn, H. J., & Solemdal, P. (1996). Physiological mechanisms of buoyancy in eggs from brackish water cod. *Journal of Fish Biology*, 48(3), 457–477. https://doi.org/10.1111/j.1095-8649.1996.tb01440.x

Tyler, C. R., & Sumpter, J. P. (1996). Oocyte growth and development in teleosts. *Reviews in Fish Biology and Fisheries*, 6, 287–318. https://doi.org/10.1007/bf00122584

van der Meeren, T., & Ivannikov, V. P. (2006). Seasonal shift in spawning of Atlantic cod (*Gadus morhua* L.) by photoperiod manipulation: Egg quality in relation to temperature and intensive larval rearing. *Aquaculture Research*, 37, 898–913. https://doi.org/10.1111/j.1365-2109.2006.01510.x

Woodhead, A. D., & Woodhead, P. M. J. (1965). Seasonal changes in the physiology of the Barents Sea cod, *Gadus morhua* L., in relation to its environment. I. Endocrine changes particularly affecting migration and maturation. *ICNAF Special Publication*, 6, 691–715.

Wright, P. J., Doyle, A., Taggart, J. B., & Davie, A. (2021). Linking scales of life-history variation with population structure in Atlantic cod. *Frontiers in Marine Science*, 8, 630515. https://doi.org/10.3389/fmars.2021.630515

Wright, P. J., Regnier, T., Gibb, F. M., Augley, J., & Devalla, S. (2018). Assessing the role of ontogenetic movement in maintaining population structure in fish using otolith microchemistry. *Ecology and Evolution*, 8, 7907–7920. https://doi.org/10.1002/ece3.4186

SUPPORTING INFORMATION

Additional supporting information can be found online in the Supporting Information section at the end of this article.